Unlocking phytoalexin biosynthesis using multigene engineering

Melissa Ly

A thesis submitted to the Faculty of Graduate Studies in partial fulfilment of the requirements for the degree of

MASTER OF SCIENCE

Graduate Program in Biology

York University

Toronto, Ontario

November 2025

ABSTRACT

Plants have evolved sophisticated defense mechanisms to balance growth and immunity, with phytoalexins and lignin playing central roles in pathogen resistance. In *Arabidopsis thaliana*, the jasmonate repressor JAZ1 and transcription factor ANAC042 act as opposing regulators of this process. The regulation of phytoalexin biosynthesis is highly complex, and manipulating individual transcription factors has generally proven insufficient to fully activate the pathway. To address this limitation, this study investigates whether the knockout of *JAZ1* in combination with the overexpression of *ANAC042* can more effectively unlock phytoalexin biosynthesis. While *JAZ1* knockout promoted systemic lignification under prolonged stress, while *ANAC042* overexpression alone did not strongly induce phytoalexins. However, their combination enhanced accumulation of hydroxyindole-3-carbonyl nitrile and monolignols. Transcriptional analysis revealed altered regulation of *WRKY33* and *MYB15*, suggesting that JAZ1 and ANAC042 are a part of a broader defense regulatory network. Growth-defense trade-offs showed growth penalties in all tested genotypes under Flg22 elicitation, except in *ANAC042* overexpression lines, where growth was unaffected by the elicitor, highlighting the metabolic costs associated with sustained immunity. Extending these findings to soybean, a dual-gene plasmid (*pGEMINI-B*) was constructed to co-overexpress two positive regulators of glyceollin biosynthesis, while silencing *GmJAZ1* genes. Collectively, these findings demonstrate that manipulating antagonistic regulatory factors simultaneously can unlock levels of phytoalexin accumulation that are unattainable through single-gene modifications. The underlying shifts in gene expression and metabolism driving this effect are unconventional and warrant deeper investigation, as elevated phytoalexin biosynthetic gene expression does not directly account for the observed increases in phytoalexin levels.

ACKNOWLEDGEMENTS

I would like to begin by expressing my sincere gratitude to everyone who has supported me throughout the course of my MSc journey, whether directly or indirectly. This work would not have been possible without the guidance, encouragement, and kindness I have received from so many people along the way. Each contribution, whether through academic advice or personal support, has been deeply appreciated and played an important role in helping me reach this stage.

First and foremost, I would like to thank my supervisor, Dr. Nikola Kovinich, for providing me this incredible opportunity to work on this project in his lab. His constructive criticism and feedback have been indispensable in shaping this project and supporting my growth as a researcher. I am especially grateful for the time and effort you have dedicated in helping me overcome challenges and to achieve this milestone.

I would also like to thank my committee members, Dr. Kathi Hudak and Dr. Andrew White (who recently retired), for your time, insightful feedback, and valuable advice. To Dr. Raymond Kwong and Dr. Satinder Brar for agreeing to be on my thesis defense.

To my lab colleagues, who I now have the privilege of calling friends. Jie and Ivan, thank you both for training me on various techniques and tolerating the countless questions I asked. To Ivan, thanks for making Arabidopsis seed sterilization a little more bearable. To Jie, I will truly miss doing hairy root transformations with you. We will always be the "Dream Team". To Sarah and Aida, I will miss our "Greenhouse Fridays," and I hope one day, we will finally manage to complete an escape room. To Izabella, our annual plant expo visits have transformed my living space into a thriving jungle, and I am so grateful for that.

To Karl, Leonardo, and Demian from Dr. Demian Ifa's lab, for kindly running my metabolite samples on your mass spectrometry instrument. I would not have been able to complete my thesis without your assistance.

I would also like to extend my deepest gratitude to my parents, to whom I dedicate this thesis. They have sacrificed immensely to give their children a better life. Thank you both for believing in me and supporting me in becoming the person I am today. I will forever be grateful for the hard work you and love you have devoted to ensuring our success.

Finally, to my fiancé, David, thank you for standing by my side through all the challenges of this journey. Your constant support has helped me overcome hardships, and I could not have asked for a better partner.

TABLE OF CONTENTS

LIST OF FIGURES

LIST OF TABLES

LIST OF ABBREVIATIONS

4OH-ICN	4-hydroxyindole-3-carbonyl nitrile
4OH-I3M	4-hydroxyindole-3-methyl
$AgNO_3$	Silver nitrate
Arabidopsis	*Arabidopsis thaliana*
ATAF1/2	*Arabidopsis thaliana* Activating Factor1/2
BAK1	BRI1-associated receptor kinase 1
CaMV	Cauliflower mosaic virus
CDS	Coding sequences
COI1-JAZ	Cornatine insensitive 1-JAZ
CPK	Calcium-dependent protein kinase
CUC2	Cup-shaped cotyledon
CYP71B15	*PAD3*
Dat	Days after treatment
ddH_2O	Double distilled water
DMSO/Mock	Dimethyl sulfoxide
EIN2	Ethylene insensitive 2
EIN3	Ethylene insensitive 3
EIN3-like 1	EIL1
FLS2	Flagellin-sensing 2
FMV	Figwort mosaic virus
GA	Gibberellin
HCl	Hydrochloric acid
IAN	Indole-3-acetonitrile
IAOx	Indole-3-acetaldoxime
ICN	Indole-3-carbonyl nitrile
I3M	Indole-3-methyl
JA-Ile	Jasmonyl-L-isoleucine
Jas	Jasmonate
Lpm	Litres per minute
LRR	Leucine-rich repeat

m/z	Mass-to-charge
M1/M2	Means of the compared group
MALDI-HRMS	Matrix-assisted laser desorption/ionization high-resolution mass spectrometry
MAPK	Mitogen-activated protein kinase
Monolignol C/C-unit	Coniferyl
Monolignol G/G-unit	Guaiacyl
Monolignol H/H-unit	*p*-hydroxyphenyl
Monolignol S/S-unit	Syringl
MPK	Mitogen-activated protein kinase
MS	Murashige and Skoog
MSw	Mean square error within the group
n	Sample size
NAC	NAM, ATAF1/2, CUC2
NAM	No apical meristem
NINJA	Novel interactor of JAZ
Nrf2	Nuclear factor E2-related factor 2
P. sojae	*Phytophthora sojae*
PAMPs	Pathogen-associated molecular patterns
Phe	Phenylalanine
PhyB	Phytochrome B
PP2Cs	Protein phosphatase 2Cs
Ppm	Parts per million
PPR	Pattern recognition receptor
ROS	Reactive oxidative species
RPM	Revolutions per minute
SA	Salicylic acid
SCF^{COI1}	Skp1-cullin-F-box protein complex
SE	Standard error
Soybean	*Glycine max*
TFs	Transcription factors

TIFY	Threonine-isolecuine-phenylalanine-tryosine
TPL	Topless
TPR	Topless-related
Trp	Tryptophan
WGE	Wall glucan elicitor
Wildtype/WT	Col-0

CHAPTER 1: INTRODUCTION

1.1.1 Phytoalexins and Relation to Stress

As sessile organisms, plants cannot escape environmental challenges and must cope with a wide range of biotic and abiotic stresses that can compromise their survival. To withstand these pressures, plants have evolved complex defense mechanisms, such as the synthesis of phytoalexins, that play a central role in mitigating defense. Phytoalexins are antimicrobial compounds produced in response to stress and derived from precursors of primary metabolic pathways (Huang and Dudareva, 2023). Unlike primary metabolites, phytoalexins do not directly contribute to reproduction, growth, or development (Sung et al., 2015). Their biosynthesis is tightly regulated, remaining largely dormant under normal conditions, but rapidly activated upon exposure to pathogens or adverse environments. During pathogen attack, phytoalexins act as a first line of defense by restricting the proliferation of invaders (Huang and Dudareva, 2023).

Biomedical studies have highlighted the medicinal potential of some phytoalexins from *Arabidopsis thaliana* (Arabidopsis) and *Glycine max* (soybean). Both species possess several distinct classes of phytoalexins that illustrate this metabolite diversity. In Arabidopsis, it was previously believed that camalexin was the sole phytoalexin produced, but later studies demonstrated that at least 12 different phytoalexins were synthesized in response to specific microbial and abiotic stresses (Monsalvo et al., 2024). Camalexin, the most well characterized phytoalexin plays a crucial role in the plant's defense against certain pathogens, and mutations in its biosynthesis pathway can leave the plant vulnerable. Aside from its antibacterial and antimicrobial properties, camalexin exhibits anticancer activity under elicitation by inducing apoptosis in leukemia infected cells (Nguyen et al., 2022; Yang et al., 2018). Camalexin is also capable of triggering apoptosis in cancerous prostate cells by promoting the accumulation of reactive oxygen species (ROS). Aggressive cancer cells with high ROS levels showed decreased viability and increased apoptosis in response to camalexin (Smith et al., 2014).While camalexin possess a broad-spectrum of defense activity, the more recently discovered 4-hydroxyindole-3-carbonyl nitrile (4OH-ICN) is known to contribute in defense to reduce further against *Pseudomonas syringae* (Rajniak et al., 2015). However, its potential to induce apoptosis in cancer cells remains unknown. Scopoletin, a coumarin, accumulates under oxidative stress and

exhibits antifungal activity (Antika et al., 2022; Tanaka et al., 1983).This compound is primarily synthesized in root tissues, where they facilitate iron uptake from the soil and help shape the root microbiome, which contributes to the overall plant health (Schmid et al., 2014).

In soybean, glyceollins function primarily as phytoalexins that inhibit the growth of microbes, including *Rhizopus oligosporus*, which highlights their contribution to protecting soybean from infection (Kalli et al., 2020). The antimicrobial activity of glyceollins is considered essential for soybean's survival against several important microbial pathogens, although the regulatory networks that control their production remain an active area of research. Beyond their ecological role in plant defense, glyceollins have also attracted interest for their pharmaceutical potential. Studies have shown that they can inhibit breast, ovarian, and prostate cancer cell growth through the modulation of estrogen receptor signaling and tumor growth pathways, as well as provide neuroprotective effects by activating antioxidant pathways such as nuclear factor E2-related factor 2 (Nrf2) and inducing expressions of *heme oxygenase 1* (Lecomte et al., 2017; Seo et al., 2018). Several of the transcription factors (TFs) that regulate glyceollin biosynthesis in soybean are homologous to those that regulate camalexin synthesis in Arabidopsis.

1.1.2 Lignin

Lignin is a phenolic polymer primarily found in the secondary cell walls of plants, consisting of several monolignol subunits. During development, lignin is systematically deposited in specific tissues including the xylem, fibers, and endodermis to enhance structural integrity, rigidity, hydrophobicity, and for water transport (Vanholme et al., 2010). In dicot plants, lignin is made from monolignols coniferyl (C) and sinapyl alcohol to give rise to guaiacyl (G) and syringyl (S) and low amounts of *p*-hydroxyphenyl (H). Its monomer composition is tightly regulated and exhibit tissue specific patterns. For example, G-units are localized in the xylem, whereas S-units are predominantly rich in angiosperms (Wang et al., 2013). While its role in providing structural support during developmental regulation is well-established, its function in defense is more dynamic (Boerjan et al., 2003; Miedes et al., 2014). Upon pathogen attack, lignin synthesis is induced to become polymerized at the infection site to create a physical barrier over open wounds to prevent further threats. Defense-induced lignin differs in biochemical makeup, varying in S-, G-, and H-unit ratios depending on what is needed for defense(Miedes et al., 2014). Free monolignols are inherently hydrophobic and are thought to function as phytoalexins,

but they also pose cytotoxic risks inside the cells by disrupting cellular homeostasis and signaling pathways (Le Roy et al., 2016; Speeckaert et al., 2020).To overcome this challenge, plants often glycosylate monolignols by converting them into water-soluble monolignol glucosides as a detoxification mechanism (Perkins et al., 2022). Another option to neutralize their monolignol toxicity is to polymerize into lignin. This could be done through laccase-mediated oxidation by reducing oxygen to water molecules (Tobimatsu and Schuetz, 2019). Monolignols also exert toxicity against pathogens. For example, in *Xanthomonas citri*, exposure to monolignols leads to aldehyde toxicity. To cope with this, the pathogen has evolved the ability to catabolize monolignols, thereby detoxifying its environment (Martim et al., 2024).

1.2 The growth-defense trade-off in plants

In plants, investment in defense, such as the activation of immune responses and the production of phytoalexins, often comes at the cost of growth and reproduction. This growth-defense trade-off reflects an evolutionary balance in resource allocation, ensuring survival under stress, while maintaining developmental and reproductive success under favourable conditions (He et al., 2022). At the molecular level, this balance is regulated by extensive hormonal crosstalk, with the jasmonate pathway serving as a key pathway that promotes defense at the expense of growth through its antagonistic interaction with phytochrome B (phyB). PhyB is a red/far-red photoreceptor that integrates environmental light cues to optimize plant architecture and stress responses. When phyB is active under red light, jasmonate-dependent defense signaling is suppressed. In contrast, inactivation of phyB allows jasmonate responses to dominate, reallocating resources toward defense (Moreno et al., 2009; Campos et al., 2016). For instance, the Arabidopsis *jasmonate ZIM-domain* (*JAZ*) quintuple mutant (*jazQ*), lacking five *JAZ*s including *jaz1*, displays constitutive defense activation and enhanced resistance to pathogens, but also suffers from significant growth impairment under stress conditions (Campos et al., 2016). Conversely, *phyB* mutants exhibit increased growth, and combining *phyB* with *jazQ* partially rescues growth defects in Arabidopsis (Campos et al., 2016). Moreover, the higher-order *JAZ* mutant, *jazD*, lacking 13 *JAZ*s including *jaz1*, exhibits even more exaggerated stunted growth (Guo et al., 2018). While there are no direct links between ANAC042 and phyB, both converge on the repression of phytochrome-interacting factor 4 (PIF4), a TF that promotes growth. ANAC042 represses *PIF4* expression in tomatoes to favour defense, while phyB

suppresses PIF4 activity to delay senescence (Shahnejat-Bushehri et al., 2017; Sakuraba et al., 2014). Tryptophan (Trp)-derived metabolism is also strongly elevated in coronatine-elicited *jazD* mutants, with increased accumulation of indole-3-methyl (I3M) and 4-hydroxyindole-3-methyl (4OH-I3M) compared to wildtype, and similar levels are observed when *jazD* is combined with *phyB* mutants (Major et al., 2020). These findings highlight the critical role of JAZ proteins in reducing defense responses to preserve metabolic balance, sustain growth, and secure reproductive success. On the contrary, ANAC042 acts as a positive regulator that promotes defense responses by activating phytoalexin biosynthesis. Such dynamic allocation strategy allows plants to maintain fitness across diverse environments by amplifying defense when required, while minimizing unnecessary metabolic costs in the absence of threats.

1.3 Phytoalexin biosynthetic pathways in Arabidopsis and soybean

The biosynthesis of phytoalexins in Arabidopsis involves the shikimate pathway, which produces tryptophan (Trp) and phenylalanine (Phe) as precursors for indole- and phenylpropanoid-derived metabolites, respectively (Figure 1). On the Trp branch, indole-3-acetaldoxime (IAOx) serves as a central intermediate for several Trp-derived phytoalexins, including camalexin and 4OH-ICN. For camalexin, IAOx is converted into indole-3-acetonitrile (IAN) by *CYP71A13* and undergoes a series of reactions where the intermediate is oxidized by *PAD3* (*CYP71B15*) to become camalexin (Schuhegger et al., 2006). For 4OH-ICN, IAOx is diverted into indole-3-cyanohydrin by *CYP71A12*, which becomes catalyzed by *FOX1* to become indole-3-carbonyl nitrile (ICN), which is subsequently hydroxylated by *CYP82C2* to become 4OH-ICN (Rajniak et al., 2015). On the Phe branch, *PAL* converts Phe into *p*-coumaric acid, which becomes *p*-courmaroyl-CoA, giving rise to monolignol H by *CCR* and *CAD*. However, other enzymes would convert *p*-coumaric acid into caffeic acid before subsequently becoming monolignol C, G, S and 5H, and scopoletin (Monsalvo et al., 2024).The type of compound synthesized depends on which biosynthetic enzyme is activated. In soybean, daidzein is a Phe-derived isoflavonoid and in response to stress, daidzein undergoes a series of reactions to give rise to three glyceollin isomers: glyceollins I, II, and III (Lin et al., 2023).

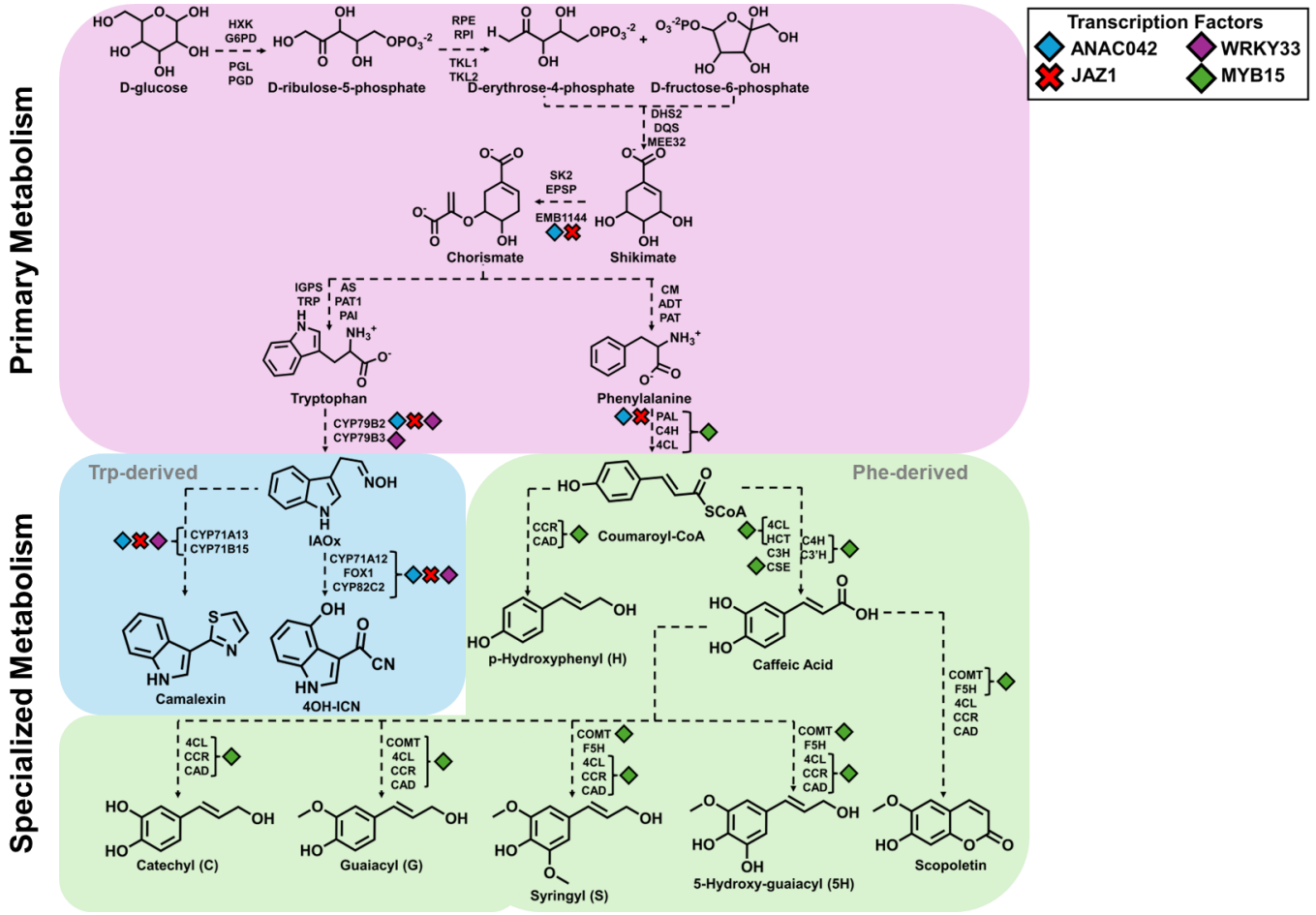

Figure 1. Biosynthetic pathways of the phytoalexins camalexin, 4OH-ICN, scopoletin, and monolignols in *Arabidopsis thaliana*. This diagram illustrates the biosynthetic pathways of these phytoalexins, beginning from primary metabolism intermediates (pink). Tryptophan-derived phytoalexins are highlighted in blue while phenylalanine-derived are in white. Metabolites are labelled in lowercase and enzymes involved in the pathways are capitalized. Transcription factors that directly regulate biosynthetic genes are indicated by symbols. ANAC042, blue diamond; JAZ1, red "X"; MYB15 and WRKY33, green and purple diamond, respectively. This figure was adapted by Monsalvo et al., 2024.

1.4 Research objectives and hypotheses

The characterization of several TFs involved in regulating phytoalexin biosynthesis has provided valuable insights into the regulatory networks controlling these medicinal compounds. However, most studies have demonstrated that manipulating a single TF alone is insufficient to

activate phytoalexin biosynthetic pathways. Recent work revealed that the overexpression of the soybean homolog of *ANAC042* failed to unlock glyceollin biosynthesis without an elicitor due to JAZ1-mediated suppression (Lin et al., 2025). JAZ1 is a negative regulator plays a pivotal role in repressing phytoalexin biosynthesis by interacting with ANAC042-type TFs. Building on these findings, I hypothesize that, if knocking out *JAZ1* derepresses the expression of phytoalexin biosynthesis genes in unelicited plants, then combining it with *ANAC042* overexpression will further promote the production of phytoalexins in Arabidopsis.

1.5 Flg22 and hormonal regulation of phytoalexin biosynthesis through *JAZ1*

Recognition of pathogen-associated molecular patterns (PAMPs) activates phytoalexin biosynthesis and other defense processes. The conserved bacterial flagellin peptide Flg22, located in the N-terminal region of flagellin, acts as a conserved PAMP that activates immune responses. Flg22 is recognized by the flagellin-sensing 2 (FLS2) receptor, a pattern recognition receptor (PRR) receptor kinase that contains a leucine-rich repeat (LRR). Loss-of-function *fls2* mutants, which disrupts the LRR domain, are unable to trigger downstream defense signaling, highlighting the importance of Flg22 perception (Chinchilla et al., 2006). Upon Flg22 recognition, FLS2 undergoes phosphorylation and associates with BRI1-associated receptor kinase 1 (BAK1), forming a receptor complex that initiates defense responses, including transcriptional activation of phytoalexin biosynthetic genes (Sun et al., 2013).

Early immune signaling also involves the production of reactive oxygen species (ROS). In Arabidopsis, ROS activate additional pathways, including mitogen-activated protein kinase (MAPK) and calcium-dependent protein kinase (CPK) cascades (Torres et al., 2002; Yoshioka et al., 2023). In the MAPK pathway, the FLS-BAK1 complex phosphorylates MAPKKK, initiating a cascade that activates mitogen-activated protein kinase 3 and 6 (MPK3/MPK6). These MAPKs are crucial for camalexin biosynthesis, as they phosphorylate TFs that regulate *CYP71A13* and *CYP71B15*. In parallel, CPK signaling is activated by extracellular ATP released from damaged cells. ATP detected PRRs triggers calcium influx, which together with ROS, acts as a secondary messenger to activate defense-related TFs (Demidchik et al., 2003; Marcec and Tanaka, 2022). Crosstalk among jasmonic acid (JA), ethylene (ET), and MAPK pathways further regulates phytoalexin biosynthesis. For example, both 1-aminocyclopropane-1-carboxylic acid, an ET

precursor and methyl jasmonate, a JA precursor, induce *ERF1* transcription, integrating ET and JA signaling with MAPK activation (Ouaked et al., 2003; Takahashi et al., 2007; Zhou et al., 2020, 2022). This convergence at MPK6 highlights the complexity of phytoalexin regulation.

The regulation of the phytoalexin biosynthesis is tightly controlled by phytohormones, with JA playing a central role. JA signaling relies on JAZ proteins. The *JAZ* gene family is a subset of the threonine-isoleucine-phenylalanine-tyrosine (TIFY) superfamily that contains two highly conserved domains: the TIFY domain near the N-terminus and the jasmonate (Jas) domain by the C-terminus (Staswick, 2008; Bai et al., 2011). Under non-elicited conditions, the TIFY domain enables JAZ proteins to interact with novel interactor of JAZ (NINJA) proteins to recruit co-repressors like topless (TPL) and topless-related (TPR) proteins. Through the Jas domain, JAZ proteins establish protein-protein interactions with NINJA, TPL, and TPR, mediating repression of multiple TFs (Pauwels et al., 2010; Pauwels and Goossens, 2011).

Following the recognition of specific PAMPs or abiotic stresses, JA is conjugated by the JA-conjugating enzyme, JAR1 to form jasmonoyl-L-isoleucine (JA-Ile). JA-Ile, along with other JA-amino acid conjugates, is perceived by the cornatine insensitive 1-JAZ (COI1-JAZ) receptor complex, which targets JAZ proteins for ubiquitin-mediated degradation by the 26S proteasome (Koo and Howe, 2009). Degradation of JAZ proteins releases TFs, allowing them to activate downstream target genes. Thus, the JA signalling pathway is a critical regulator of defense responses, including phytoalexin biosynthesis. Like other JAZ proteins, JAZ1 negatively regulates the JA signaling pathway by inhibiting MYC2, a key transcriptional regulator of the JA responses (Chini et al., 2007). For example, MYB34 regulates the JA pathway and interacts with *CYP72B2* and *CYP79B3* to convert Trp into IAOx (Yi et al., 2016). Silencing of *jaz1* significantly upregulated *ANAC042* and *WRKY33* expression, suggesting that JAZ1 normally suppresses *ANAC042* transcription (Makhazen et al., 2021). However, closer inspection of the promoter sequences of *JAZ1* revealed multiple W-box sequences, suggesting that WRKY33 may target JAZ1 to repress their activity, rather than JAZ1 inhibit WRKY33's activity (Birkenbihl et al., 2012). Beyond biotic stress, JAZ1 is also involved in abiotic stress responses such as cold tolerance. JAZ1 directly interacts with ICE1 and ICE2, TFs that activate cold-responsive genes, thereby repressing their function under non-elicited conditions. During cold stress, elevated JA levels promote JAZ1 degradation, releasing both MYC2 and ICE proteins to activate JA and cold

tolerance pathways, respectively (Hu et al., 2013). In addition to its role in JA signaling, JAZ1 mediates crosstalk with other hormonal pathways. In the ET signaling pathway, JAZ1 interacts with ethylene insensitive 3 (EIN3) and its closest homolog EIN3-like 1 (EIL1), TFs downstream of *ethylene insensitive 2* (*EIN2*) gene, to inhibit their activity and thereby prevent ET-dependent induction of phytoalexins such as camalexin (Alonso et al., 2003; Chao et al., 1997; Solano et al., 1998; Song et al., 2014; Zhu et al., 2011). Normally, ET modulates plant growth and defense by suppressing JA-induced wound responses, while JA suppresses ET-induced apical hook formation (Memelink, 2009; Turner et al., 2002). Similarly, abscisic acid (ABA) signaling maintains JAZ protein stability and antagonizes JA signaling. For example, ABA and MYC interact to repress JA biosynthesis, while pathogens such as *Pseudomonas syringeae* exploit ABA-induced protein phosphatase 2Cs (PP2Cs) to dephosphorylate MPK3/MPK6, dampening defense responses (Anderson et al., 2004; Mine et al., 2017; Mohr and Cahill, 2003). Any reductions in endogenous ABA levels have been observed during the onset of glyceollin biosynthesis, highlighting the antagonism between ABA and phytoalexin production, and *JAZ* is upregulated by ABA (Mine et al., 2017; Mohr and Cahill, 2003).

In soybean, silencing *GmJAZ1* promotes glyceollin accumulation in transgenic hairy roots elicited with wall glucan elicitor (WGE) derived from *Phytophthora sojae* (*P. sojae*) (Lin et al., 2023; Lin et al., 2025). During infection, *P. sojae* expresses the Avh94 effector protein, which interacts with GmJAZ1 and GmJAZ2 proteins to prevent ubiquitin-mediated degradation by the 26S proteasome (Zhou et al., 2022). Notably, prolonged stress (six days) involving ABA or dehydration strongly upregulates multiple *GmJAZ1* variants and represses glyceollin production, whereas short-term (24 hours) stress, which has traditionally been the focus of most studies, does not trigger this repression (Lin et al., 2025). This distinction highlights a critical gap in our understanding of phytoalexin regulation that JAZ1 does not exert immediate repression after elicitation, but instead functions during sustained stress, thereby shaping long-term phytoalexin regulation.

1.6 Positive regulators of phytoalexin biosynthesis

Several TFs act as positive regulators that directly activate the biosynthetic genes of phytoalexin in response to stress signals. In Arabidopsis and soybean, these include

ANAC042/GmNAC42-1, WRKY33, MYB15/GmMYB29A2, and GmHSF6-1. The TF WRKY33, serves as a master regulator of camalexin biosynthesis in Arabidopsis through MAPK-mediated activation (Mao et al., 2011; Zhou et al., 2020). While MYB15 controls monolignol and scopoletin biosynthesis in Arabidopsis, its soybean homolog, *GmMYB29A2*, activates glyceollin biosynthesis (Chezem et al., 2017; Jahan et al., 2020). Similarly, soybean heat shock factor, GmHSF6-1, has been shown to activate glyceollin pathway genes following elicitation (Lin et al., 2023). Although these factors highlight the complexity of transcriptional control in specialized metabolism, ANAC042 remains the most directly linked to the regulation of multiple phytoalexins and represents a key node in connecting JA signaling with defense metabolite production.

ANAC042 is a member of the NAC [NAM (No Apical Meristem), ATAF1/2 (Arabidopsis thaliana Activating Factor), and CUC2 (Cup-shaped Cotyledon)] gene family, one of the largest TF families of plants. Members of this family contain a highly conserved NAC domain at the N-terminus and a transcriptional regulatory region at the C-terminus. The NAC domain consists of 150 amino acids and is responsible for DNA binding (Chen et al., 2011; Liu et al., 2023).

Beyond its role in phytoalexin biosynthesis, ANAC042 has been implicated in regulating organ longevity. Characterized as a ROS-responsive TF, ANAC042 extends organ lifespan in Arabidopsis. Under oxidative stress, its expression is strongly induced, leading to the activation of stress-protective genes such as *DREB2A* and *HSFA3*, which functions as heat shock-responsive and heat shock TF genes, respectively (Schramm et al., 2008; Suzuki et al., 2011; Wu et al., 2012; Yoshida et al., 2008). At the same time, ANAC042 represses *GA3ox1* and *DWF4*, two key genes involved in gibberellin and brassinosteroid biosynthesis, resulting in reduced growth rates and delayed senescence (Shahnejat-Bushehri et al., 2012). In addition to mediating stress tolerance and longevity, ANAC042 contributes to defense by directly regulating the biosynthesis of multiple phytoalexins (Monsalvo et al., 2025). ANAC042 was also linked to camalexin biosynthesis, where it upregulates the transcription of biosynthetic genes, such as *CYP71A12, CYP71A13,* and *CYP71B15* upon elicitation (Saga et al., 2012; Figure 1). The expression levels of *CYP71A13* and *CYP71B15* were downregulated in loss-of-function *anac042* mutants, reinforcing ANAC042's role in regulating camalexin. Recent studies have shown that ANAC042 regulates phytoalexins beyond camalexin biosynthesis. ANAC042 upregulates *FOX1*

and *CYP82C2* genes upon Flg22 elicitation, indicating a role in 4OH-ICN biosynthesis. Notably, ANAC042 also upregulates *PAL*, the key biosynthetic gene involved in synthesizing Phe-derived phytoalexins and this was also confirmed with systemic lignification in *ANAC042* overexpression lines (Monsalvo et al., 2025; Figure 1). Previous attempts to manipulate the *ANAC042* homolog, *GmNAC42-1* in soybean, by overexpression failed to fully activate the glyceollin biosynthesis pathway (Jahan et al., 2019). In Arabidopsis, ANAC042 activity is also mediated by JAZ repressors. In a loss-of-function *jaz1* mutant, *ANAC042* expression levels increase significantly, suggesting that JAZ1 negatively regulates ANAC042 (Saga et al., 2012; Figure 2). This conserved role of JAZ1 in repressing ANAC042 was further confirmed when homologs of *JAZ1* in three different plant species (Lin et al., 2025). Arabidopsis, grapevine, and soybean demonstrated direct interaction with their respective NAC42 TF (Lin et al., 2025). The interaction with JAZ1-like prevents ANAC042 from interacting with biosynthetic genes involved in phytoalexin production, which highlights that JAZ1- and ANAC042-type proteins have opposing roles in the regulation of phytoalexin biosynthesis (Lin et al., 2025).

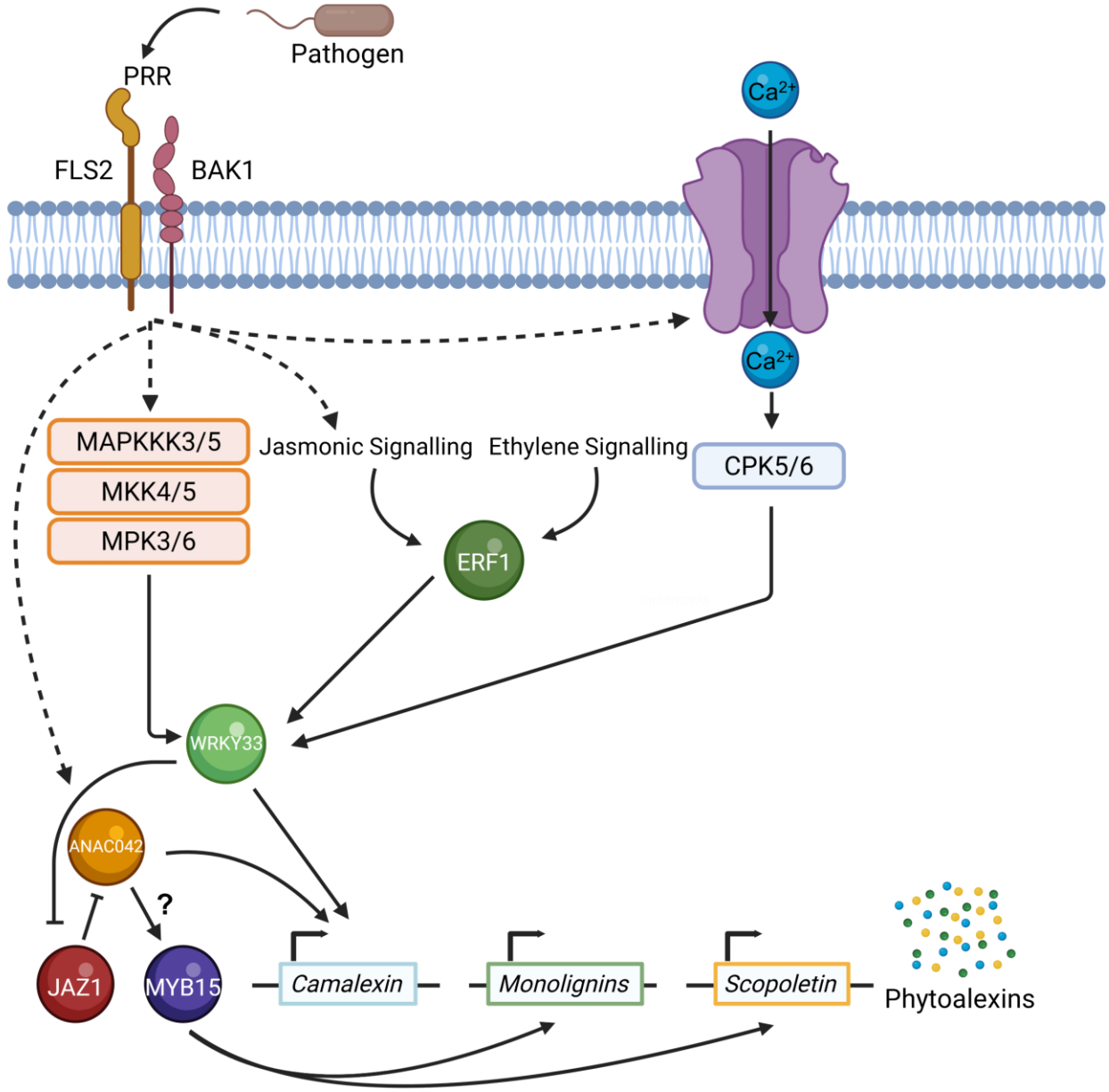

Figure 2. Protein and DNA interactions among transcription factors regulating camalexin, scopoletin, and lignin biosynthesis in *Arabidopsis thaliana*. This diagram depicts the protein-protein interactions among key transcription factors involved in the regulation of camalexin, scopoletin, and lignin biosynthesis. The interactions between transcription factors such as WRKY33, MYB15, ANAC042, and JAZ1 are illustrated, highlighting their roles in modulating the expression of genes within the respective biosynthetic pathways. Solid lines indicate direct interactions, while dashed lines suggest potential or indirect interactions. This figure was created by the author for this master's thesis.

CHAPTER 2: MATERIALS AND METHODS

2.1 Cloning

For the Arabidopsis construct, the coding sequence (CDS) of *ANAC042* was PCR amplified and cloned into the entry vector, *pENTR D-TOPO* (TOPO-U14-B03) within *Escherichia coli* that was purchased from the Arabidopsis Biological Resource Center (Columbus, OH, USA). The *ANAC042* CDS was subsequently transferred into the destination vector, *pGWB2* using LR Clonase enzyme mix (Invitrogen, ON, Canada) in *Escherichia coli*. The *pGWB2* vector is an overexpression vector encoding a viral cauliflower mosaic virus (CaMV) *35S* promoter positioned upstream of a Gateway recombination cassette. The integration of *ANAC042* CDS was screened by colony PCR and confirmed by Sanger sequencing (The Centre for Applied Genomics, ON, Canada) using gene-specific primers, cANACf/cANACr (Table S1). From *Escherichia coli, ANAC042* in *pGWB2* was transformed into *Agrobacterium tumefaciens* strain *GV3101*.

2.2 Plant Growth and Elicitation

Arabidopsis seeds of Col-0 (CS60000), *jaz1-1* (SALK_011957C), and *anac042-1* (CS104919) were purchased from the Arabidopsis Biological Resource Center (Columbus, OH, USA). For sterilization, seeds were submerged in 70% ethanol to remove debris and soil, followed by vigorous shaking in 10% commercial bleach for five minutes. They were then washed several times with sterile double distilled water (ddH_2O) prior to plating. For selection of transgenic lines, seeds were plated on solid Murashige and Skoog (MS) selection medium pH 5.8 containing 1% sucrose (w/v), 2.5g/L Gelzan, 2.5mL/L 1000X MS vitamins, 500 mg/L timentin (Gold Biotechnology, MO, USA), and 50 mg/L kanamycin and hygromycin (Gold Biotechnology, MO, USA). Plates were cold-stratified in the dark at 4°C for two days prior to being placed under cool-white T5 fluorescent lights at 100 $\mu E\ m^{-2} \cdot s^{-1}$ for five-six hours at 22°C. Plates were then transferred to dark for two days to accelerate selection and subsequently returned to 22°C day/20°C night under a 12-hour light/dark photoperiod (Denoux et al. 2008). Three days later, seedlings displaying elongated hypocotyls and bright green leaves were considered transformed and were transferred to non-selective plates and grown for 7-14 days

under light (100 μE $m^{-2} \cdot s^{-1}$) at 22°C until the first true leaves fully developed. Selected seedlings were transferred to soil and grown to maturity under 16/8-hours light (100 μE $m^{-2} \cdot s^{-1}$)/dark at 23°C/ 21°C, respectively. Harvested seeds were desiccated overnight under vacuum then stored with Drierite desiccant (Fisher Scientific, MA, USA) at room temperature in the dark until use. The same process was repeated for the T2 generation, and their seeds (T3 progeny) were harvested. To identify homozygous T2 lines, the T3 seeds were subjected to the same treatments as in previous generations, including seed sterilization, germination on antibiotic-specific medium, and selection. Lines in which all seedlings exhibited elongated hypocotyls and bright green leaves were considered homozygous. For each genotype, five lines were analyzed using the lignin assay. The line demonstrating the most uniform lignin staining patterns in the leaves and stems were selected for experiments measuring phytoalexin accumulation and their corresponding biosynthetic gene expression levels.

For elicitation, Arabidopsis seedlings were treated as described by (Parasecolo et al., 2025). Briefly, 10 day-old seedlings (n = 15) were placed in 12 well plates and immersed in 1 mL liquid MS medium pH 5.8 with 1% sucrose, MS vitamins, containing 5μM Flg22 (PhytoTech Lab, KS, USA) and dimethyl sulfoxide (DMSO/mock) (ThermoFisher, MA, USA). In total, three biological replicates were conducted for each genotype and each treatment. The plates were sealed with Parafilm to maintain humidity and incubated at 80 revolutions per minute (rpm) on a platform orbital shaker. Six days after treatment, 1 mL fresh liquid MS was supplemented into each well to prevent dehydration. 10 days post-treatment, the liquid media were harvested for metabolite extraction, and the plants were flash frozen in liquid nitrogen and stored at -80°C until used for RNA extraction.

2.3 Transforming *Arabidopsis thaliana*

Once the secondary bolts of genotypes, Col-0 (Wildtype/WT), *jaz1-1*, and *anac042* had reached two-to-10 cm in height, siliques were removed and any unopened floral meristems were transformed using the dip method (Clough and Bent, 1998). Bolts were submerged in solution containing *Agrobacterium tumefaciens* strain *GV3101* carrying *ANAC042-pGWB2*. Plants were covered overnight with plastic wrap to maintain humidity and overlaid with paper towel to reduce light exposure. After 16 hours, the plants were uncovered and grown until the siliques dried and matured. Seeds were harvested and stored as described above.

2.4 Lignin Staining Assay

Lignin staining was performed as described by (Chezem et al., 2017). Briefly, 10 day-old seedlings (n = 10) grown on solid MS medium were transferred to 12 well plates containing 1 mL liquid MS medium and treated with either 5 μM Flg22 or dimethyl sulfoxide (DMSO). These seedlings were then placed on an orbital platform shaker and incubated at 22°C day/20°C night under a 12 hour light/dark photoperiod at 80 rpm. Six days after treatment, the medium was replenished with liquid MS, and seedlings were returned to the growth chamber with shaking at 80 rpm for an additional four days. After incubation, the liquid MS medium was replaced with a fixative solution of a 3:1 mixture of 95% ethanol and acetic acid for a total of three rounds: for the first round of fixative solution, the seedlings were vacuum infiltrated for five minutes and subsequently twice for one hour until the leaves became translucent. Seedlings were then washed for 30 minutes with 75% ethanol, then 50% and finally overnight with sterile ddH_2O. Lignin staining was performed by incubating seedlings in 1% (w/v) phloroglucinol (Fisher Scientific, MA, USA) in 50% (v/v) hydrochloric acid (HCl) for five minutes. Images were captured immediately after staining using a Wild M3B stereomicroscope (Leica, HE, Germany).

2.5 Dry Weight Measurements

After 10 days of treatment with DMSO and 5 μM Flg22, Arabidopsis seedlings (n = 15 per biological replicate) were gently rinsed with ddH_2O using a Rapid-Flow filtration system (Thermo Scientific, MA, USA) to remove any residual medium. Seedlings were then transferred to pre-weighed 2 mL Eppendorf tubes, flash frozen in liquid nitrogen, and lyophilized at 0.2 torr using a BenchTop Pro (SP Scientific, PA, USA) for three days. Once dried, the tubes containing the seedlings were weighed using an ME104E analytical balance (Mettler Toledo, OH, USA). The dry weight of seedlings was determined by subtracting the pre-measured weight of the empty tube from the combined weight of the tube and seedlings. For each genotype, three independent biological replicates were analyzed along with two technical replicates per biological replicate. The dry seedlings were then stored in a -80°C ultra-low freezer until RNA extraction.

2.6 Metabolite Analysis by MALDI-HRMS

The liquid media harvested after 10 days of treatment was extracted twice by vortexing with half

volume of ethyl acetate followed by centrifugation at 13,000 g for 10 minutes. The combined ethyl acetate extracts were dried under a stream of nitrogen gas (N-Evap 111, Organomation, MA, USA) at six litres per minute (lpm) airflow. The dried extracts were dissolved in 20 µL/mg fresh tissue with methanol: H_2O: acetic acid (80:20:1) for mass spectrometry analysis.

Metabolite extracts were analyzed using matrix-assisted laser desorption/ionization high-resolution mass spectrometry (MALDI-HRMS) using a Q Exactive mass spectrometer (Thermo Scientific, MA, USA) equipped with a dual MALDI/ESI ion source (Spectroglyph, WA, USA), as described by (Parasecolo et al., 2025).

Samples were analyzed with a resolving power of 70,000 at 200 mass-to-charge (*m/z*), a maximum injection time of 200 ms, and an *m/z* range of 100–1000. Ion intensities were extracted using Thermo Xcalibur Qual Browser based on the exact mass of each compound (Table S2). Three biological and technical replicates of 10-day-old seedlings were analyzed per treatment.

2.7 RNA Extraction and Gene Expression Analysis

Snap-frozen seedlings were lyophilized again for two hours at 0.2 torr using a BenchTop Pro (SP Scientific, PA, USA). The seedlings were ground into a fine powder using an MM400 mixer mill (Retsch, CT, USA) for two minutes at 30/s. Total RNA was extracted using the HiPure Total RNA Mini Kit (GeneBio Systems, ON, Canada), quantified with a NanoDrop ND-1000 spectrophotometer (ThermoFisher Scientific, MA, USA), and treated with DNase I (Invitrogen, ON, Canada) to remove genomic DNA. cDNA was synthesized using a kit following the manufacturer's instructions (GeneBio Systems, ON, Canada). The quality of the cDNA was validated by RT-PCR using primers cActin2F/cActin2R and visualized on 1% agarose gel. qRT-PCR was performed using a CFX Opus 96 Real-Time PCR System (Bio-Rad Laboratories, ON, Canada) and the GB-AMP^{TM} SYBR Green Supermix (GeneBio Systems, ON, Canada). Gene expression was measured using the formula Expression = $2^{-[\mathrm{Ct(gene)-Ct}(\textit{ACTIN2})]}$, where *UBIQUITIN10* served as a reference gene. Primers are listed in (Table S1).

2.8 Accession Numbers

Table 1. The Arabidopsis transcription factor names with their corresponding accession number, a unique identifier to track different variations of a protein sequence.

TF Name	Accession Numbers
ANAC042	AT2G43000
WRKY33	AT2G38470
MYB15	AT3G23250
JAZ1	AT1G19180
EMB1144	AT1G48850
CYP79B2	AT4G39950
CYP71A12	AT2G30750
FOX1	AT1G26380
CYP82C2	AT4G3197
CYP71A13	AT2G30770
CYP71B15	AT3G26830
SK1	AT2G21940
PAL	AT2G37040

2.9 Statistics

For qRT-PCR and MS measurements, single-factor ANOVA and Tukey post-hoc test were applied to determine whether significant differences existed between the group means across treatments and genotypes at $\alpha = 0.05$ and $p < 0.05$. ANOVA values were computed using the Data Analysis tool of Excel (Microsoft Office Professional Plus 2019), and Tukey values were calculated using the formula $(M1-M2)/(\sqrt{(MSw(1/n))})$, where *M1* and *M2* are the means of the compared groups, *MSw* is the mean square error within the group, and *n* represents the sample size. Paired comparisons were performed using Student's t-test in Excel.

CHAPTER 3: RESULTS

3.1 Time-course analysis reveals JAZ1 knockout of lignification

Previous studies showed that expression of soybean *GmJAZ1* genes was unaffected by dehydration or ABA treatments at 24 hours, but expression increased after prolonged exposure (six days). Silencing *GmJAZ1* stimulated glyceollin I, II, and III accumulation after six days of dehydration stress, the time that *GmJAZ1*s were upregulated in wildtype. These findings indicate that *JAZ1* genes have a role in ABA-stimulated chronic stress responses (Lin et al., 2025). Since ABA has a putative role in repressing phytoalexin synthesis, we hypothesized that *JAZ1* has a role in the chronic repression of phytoalexin synthesis. To test this, we conducted a time-course analysis of lignin staining in the loss-of-function mutant *jaz1-1* upon Flg22 treatment. As a control, we included the *fls2* mutant that lacks Flg22 perception, thus no lignin staining should be observed in this mutant.

Under mock treatment, wildtype showed no lignification until 10 days after treatment (dat) (Figure 3A). Lignin deposition was localized to the stem. By contrast, *jaz1-1* showed lignification in the stem two days earlier that persisted 10 dat (Figure 3A). Flg22 elicitation of the wildtype triggered systemic lignification (roots, stems, and leaves) at two dat, which receded thereafter (Figure 3B). By contrast, at two dat *jaz1-1* exhibited lignin deposition restricted to the stem spread at four dat, partially diminished at six to eight dat, then became systemic by 10 dat. These findings demonstrate that JAZ1 suppresses lignification at later timepoint (10 days) in response to Flg22.

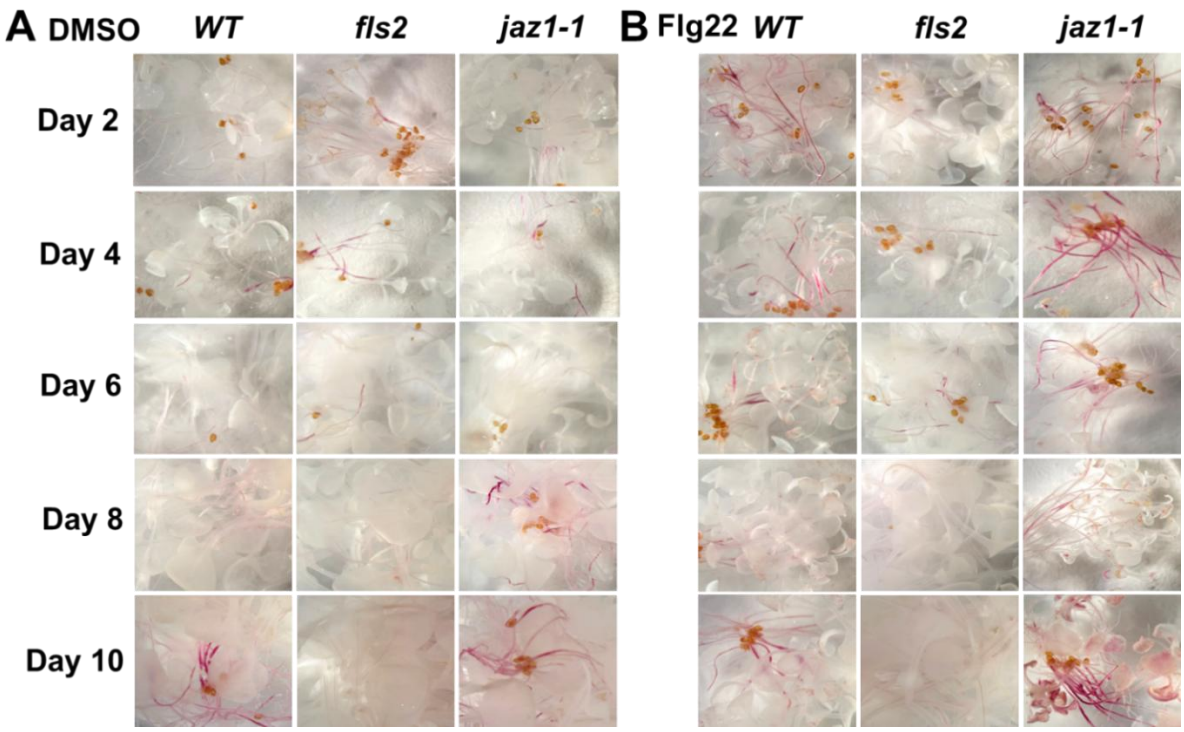

Figure 3. Time course of lignin staining using phloroglucinol-HCl staining. 10 day-old seedlings of genotypes *Col-0*, *fls2*, and *jaz1-1* were treated under **(A)** non-elicited (DMSO) and **(B)** Flg22-elicited conditions for 10 days. Images were captured at two-day intervals. Red/pink colouration indicate localization of lignin in seedlings, $n = 15$.

3.2 Simultaneous overexpression of *ANAC042* and *JAZ1* knockout unlocks the expression of the phytoalexin 4OH-ICN

Previous studies established that ANAC042 positively regulates the expression of both Trp- and Phe-derived phytoalexins (Saga et al., 2012; Monsalvo et al., 2025). In contrast, JAZ1 binds ANAC042 and suppresses its activity to negatively regulate JA-induced biosynthesis of Trp-derived phytoalexins under non-elicited conditions (Makhazen et al., 2021). Based on these findings, we hypothesized that repressing the expression of *JAZ1* would enhance phytoalexin biosynthesis, and that combining *JAZ1* knockout with *ANAC042* overexpression would further amplify this effect. To test this, we analyzed Trp- and Phe-derived phytoalexin accumulation in the *jaz1-1* null mutant overexpressing *ANAC042* via the viral 35S promoter (*p35S::ANAC042*).

p35S::ANAC042 jaz1-1 showed significantly enhanced accumulation of 4OH-ICN under mock conditions, achieving 12.3-fold greater amounts than the wildtype (Figure 4A). By contrast, both *jaz1-1* and *p35S::ANAC042 anac042-1* failed to increase the levels of 4OH-ICN compared to wildtype. Phytoalexin biosynthesis occurs transiently in plant tissues. The greatest amounts of 4OH-ICN in Flg22-treated wildtype occurred 12 hours after treatment. In comparison, non-elicited *p35S::ANAC042 jaz1-1* had 11.6-fold greater amounts of 4OH-ICN compared to 12 hour elicited wildtype (Figure 4C). Treatment with Flg22 further amplified this pattern, with *p35S::ANAC042 jaz1-1* accumulating 40-fold more 4OH-ICN than elicited wildtype, representing a three-fold increase over its mock-treated counterpart (Figure 4A). Despite showing significantly elevated 4OH-ICN accumulation, elicited *p35S::ANAC042 jaz1-1* failed to enhance the expression of biosynthetic genes *CYP71A12, FOX1,* and *CYP82C2* (Figure 4D). These results demonstrate that simultaneous *JAZ1* knockout with *ANAC042* overexpression can bypass conventional elicitor signaling to unlock high levels of 4OH-ICN accumulation, perhaps through a noncanonical regulatory mechanism.

In the Phe biosynthetic pathway, *jaz1-1* and *p35S::ANAC042 jaz1-1* maintains wildtype levels of monolignol C under mock treatment. Following Flg22 treatment, *p35S::ANAC042 jaz1-1* accumulated 5.5-fold more monolignol H compared to wildtype and was the only genotype that induced monolignol G and S (Figure 4B). These metabolic shifts correlate with the upregulation of *PAL1* in untreated *p35S::ANAC042 jaz1-1*, which reduced to wildtype levels upon elicitation (Figure 4D). Additionally, lignin staining revealed lignin solely present in stems of wildtype and an ectopic lignin deposition pattern for *p35S::ANAC042 jaz1-1*, where the entirety of the seedlings was stained (Figure 4E). In contrast to the upregulation of 4OH-ICN and a few monolignols, all other phytoalexins were not significantly upregulated in other genotypes: *jaz1-1* and *p35S::ANAC042 anac042-1*.

Shifts in phytoalexin accumulation patterns and the expressions of their biosynthetic genes in both Trp- and Phe-derived pathways prompted us to investigate whether precursor availability might explain the observed metabolite profiles. In *p35S::ANAC042 jaz1-1*, IAOx levels were 4.2-fold higher than in wildtype, while caffeic acid showed a 7.4-fold increase under non-elicited conditions. Flg22 induction further enhanced IAOx and caffeic acid accumulation in *p35S::ANAC042 jaz1-1* by 8.2- and 4.8-fold, respectively (Figure 4A and 4B). However,

chorismate, Trp, and Phe were undetectable (Figure S1). We then examined the biosynthetic gene expression from the phenylpropanoid pathway. *EMB1144* expression increased 1.5-fold in *p35S::ANAC042 jaz1-1*, but *SK2* remained at wildtype levels. Conversely, *SK1* expression was reduced by 1.8-fold in *p35S::ANAC042 jaz1-1* compared to wildtype (Figure 4D). Following Flg22 elicitation, *p35S::ANAC042 jaz1-1* maintained wildtype expression of *EMB1144* and *SK2*, but 1.3-fold reduction in *SK1* (Figure 4D). These findings establish that knocking out *JAZ1* and simultaneously overexpressing *ANAC042* deregulates the production of select phytoalexins, namely 4OH-ICN, through a mechanism distinct from the canonical regulation of phytoalexin biosynthesis.

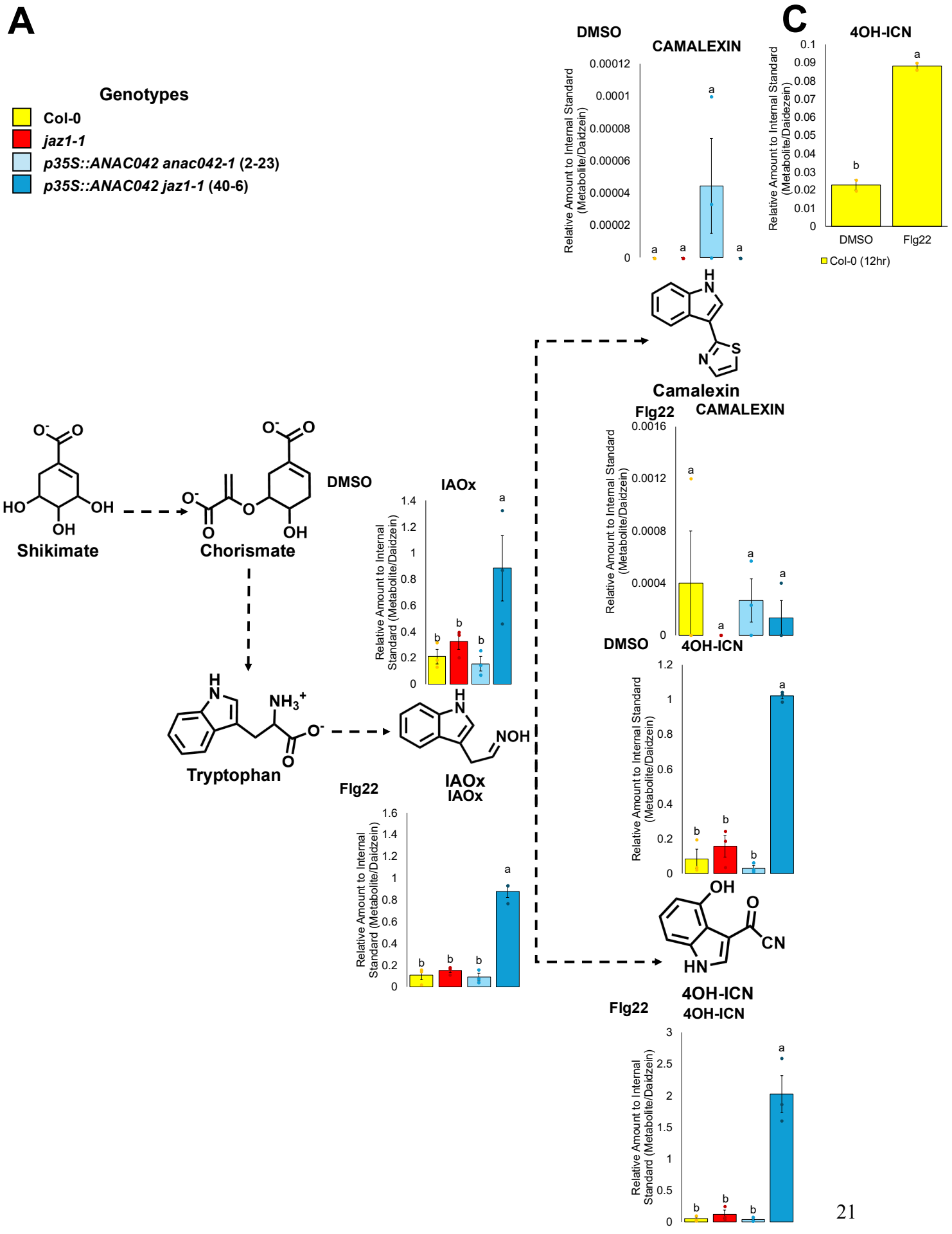
A
Genotypes
Col-0
jaz1-1
p35S::ANAC042 anac042-1 (2-23)
p35S::ANAC042 jaz1-1 (40-6)
Shikimate
Chorismate
Tryptophan
IAOx
Camalexin
4OH-ICN
DMSO
Flg22
CAMALEXIN
IAOx
4OH-ICN
Relative Amount to Internal Standard (Metabolite/Daidzein)
C
4OH-ICN
Relative Amount to Internal Standard (Metabolite/Daidezein)
DMSO
Flg22
Col-0 (12hr)

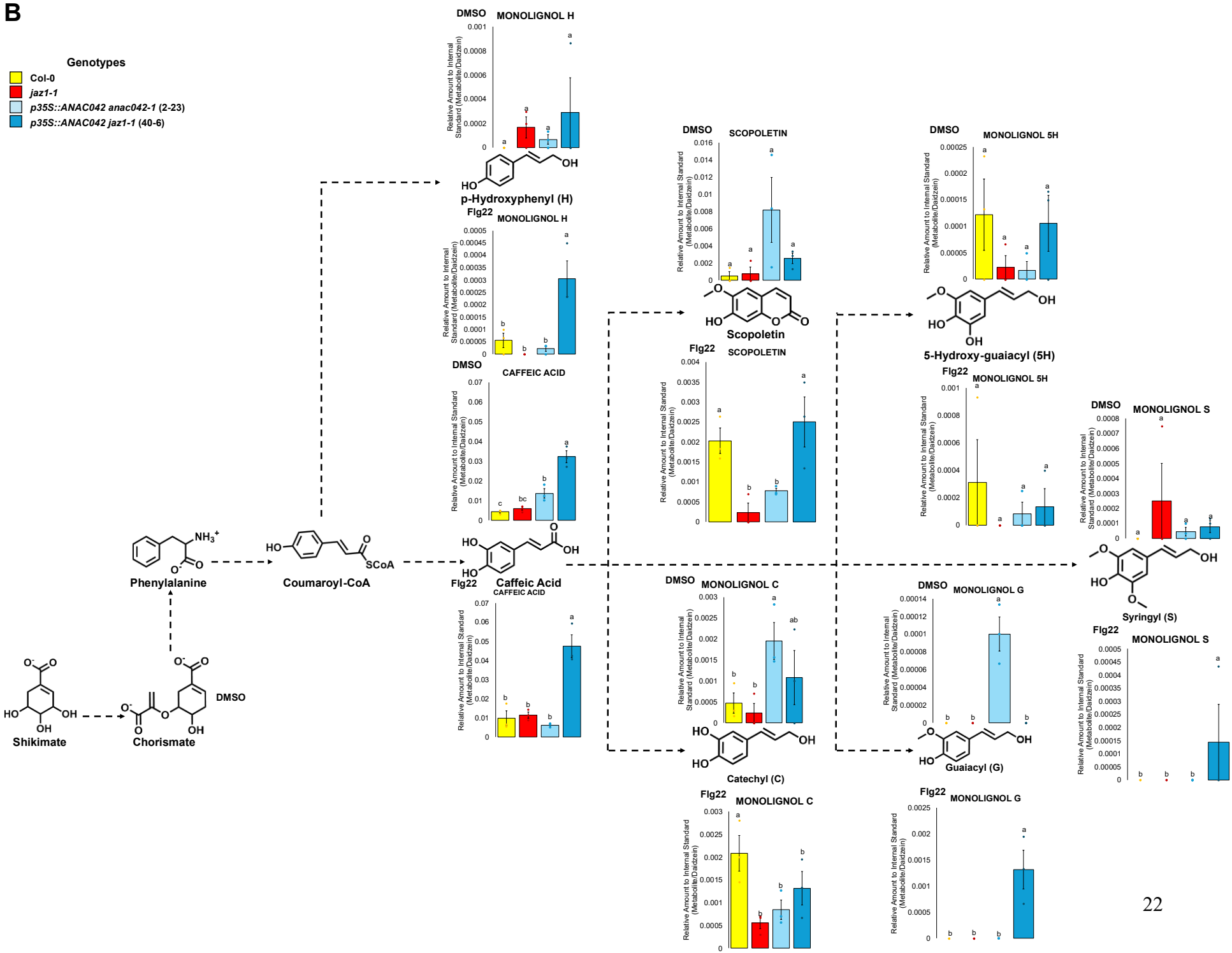
B
Genotypes
Col-0
jaz1-1
p35S::ANAC042 anac042-1 (2-23)
p35S::ANAC042 jaz1-1 (40-6)
DMSO
MONOLIGNOL H
Relative Amount to Internal Standard (Metabolite/Daidzein)
p-Hydroxyphenyl (H)
Flg22
MONOLIGNOL H
SCOPOLETIN
Scopoletin
MONOLIGNOL 5H
5-Hydroxy-guaiacyl (5H)
CAFFEIC ACID
Caffeic Acid
MONOLIGNOL C
Catechyl (C)
MONOLIGNOL G
Guaiacyl (G)
MONOLIGNOL S
Syringyl (S)
Phenylalanine
Coumaroyl-CoA
Shikimate
Chorismate

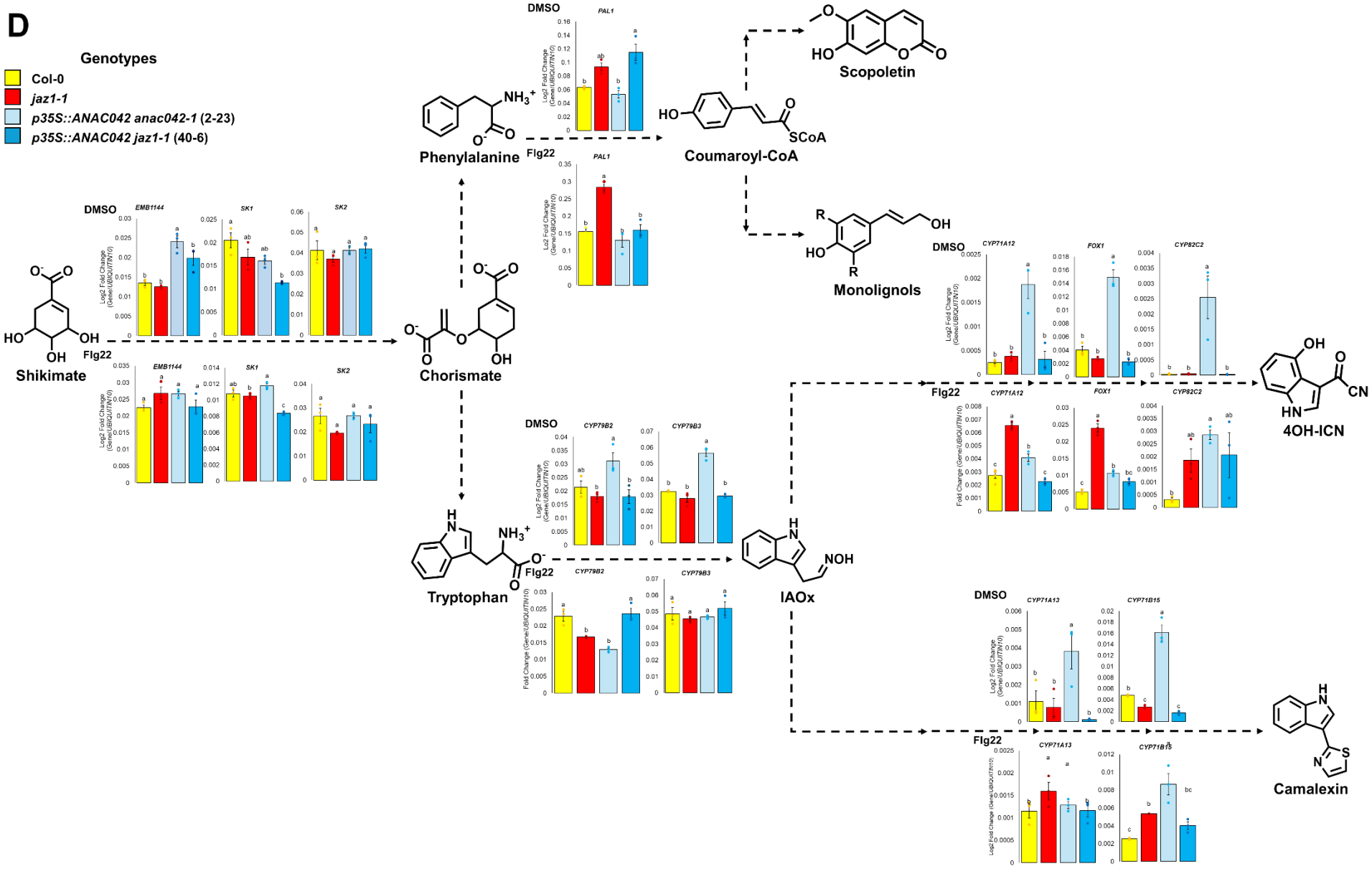
D
Genotypes
Col-0
jaz1-1
p35S::ANAC042 anac042-1 (2-23)
p35S::ANAC042 jaz1-1 (40-6)
Shikimate
Chorismate
Phenylalanine
Tryptophan
Coumaroyl-CoA
Scopoletin
Monolignols
IAOx
4OH-ICN
Camalexin
DMSO
Flg22
PAL1
EMB1144
SK1
SK2
CYP79B2
CYP79B3
CYP71A12
FOX1
CYP82C2
CYP71A13
CYP71B15

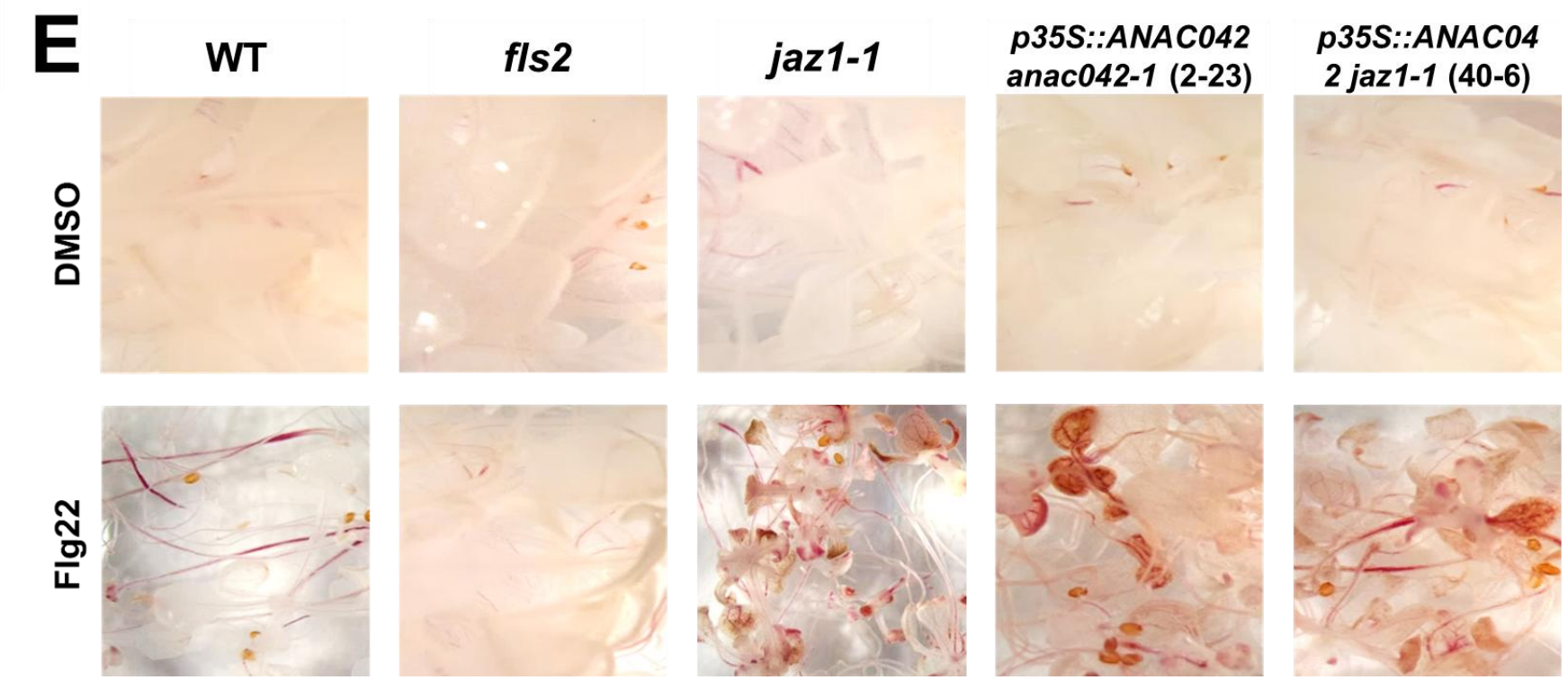

Figure 4. *ANAC042* overexpression in *jaz1-1* increases the accumulation of select tryptophan- and phenylalanine-derived phytoalexins. **(A)** Tryptophan- and **(B)** phenylalanine-derived metabolite profiles in Arabidopsis seedling extracts treated for 10 days with/without Flg22 and quantified by MALDI-HRMS. Different letters show significant differences by single factor ANOVA, Tukey post-hoc test, $p < 0.01$, $\alpha = 0.05$. Error bars represent standard error (SE), $n \geq$ three per treatment. **(C)** 4OH-ICN metabolite accumulation in Col-0 Arabidopsis seedling extracts treated for 12 hours with/without Flg22 and quantified by MALDI-HRMS. Different letters show significant differences by single factor ANOVA, Tukey post-hoc test, $p < 0.01$, $\alpha = 0.05$. Error bars represent SE, $n \geq$ three per treatment. **(D)** Expression of primary metabolic, tryptophan- and phenylalanine-derived pathway genes in Col-0, *jaz1-1*, *p35S::ANAC042 anac042-1* (2-23), and *p35S::ANAC042 jaz1-1* (40-6) Arabidopsis seedlings after 10 days of treatment,

quantified by qRT-PCR. Different letters show significant differences by single factor ANOVA, Tukey post-hoc test, $p < 0.01$, $\alpha = 0.05$. Error bars represent SE, n = four per treatment. **(E)** Phloroglucinol-HCl staining of lignin deposition under 16x magnification of 10 day treated Arabidopsis seedlings with/without Flg22, n = 15.

3.3 Simultaneous *ANAC042* overexpression and *JAZ1* knockout regulate phytoalexin transcription factor networks

Plants employ sophisticated multi-layered signaling pathways to activate defense programs against pathogens. These involve ROS generation, MAPK and CDPK cascades, and biosynthesis of defense-related phytohormones. Phytoalexin TFs act as a point of convergence of these signaling pathways and direct activate the expression defense genes such as other transcription factors and phytoalexin biosynthetic genes (Ton et al., 2002; Wang et al., 2020; Zhou et al., 2022). Previous studies demonstrated that soybean GmJAZ1-9 represses GmNAC42-1-mediated transactivation of glyceollin biosynthetic gene promoters by blocking its binding to DNA (Lin et al., 2025). Also, *MYB15* expression is reduced in *anac042-1* mutants but restored in *ANAC042* overexpression (Monsalvo et al., 2025). Thus, NAC42-type TFs exhibit multiple layers of regulation of the activation of phytoalexin biosynthetic genes.

To investigate further the deregulation of phytoalexins, we analyzed whether *ANAC042* overexpression combined with *JAZ1* knockout affects the expression of other phytoalexin TF genes using qRT-PCR. *WRKY33* expression increased by 2.2-folds in untreated *p35S::ANAC042 anac042-1*, but remained unchanged in *jaz1-1* and *p35S::ANAC042 jaz1-1* (Figure 5A). Similarly, *MYB15* expression were 7.1-fold higher in *p35S::ANAC042 anac042-1* compared to wildtype, while remained unchanged in *jaz1-1* and *p35S::ANAC042 jaz1-1* (Figure 5A). *JAZ1* expression was unaltered in the *p35S::ANAC042 jaz1-1* seedlings, but upregulated by 4.7-folds in *p35S::ANAC042 anac042-1*. *ANAC042* transcript levels were significantly increased in both *ANAC042* overexpression lines (Figure 5A). Upon Flg22 elicitation, *p35S::ANAC042 jaz1-1* reduced *WRKY33* and *MYB15* by 1.4- and 4.9-fold, respectively (Figure 5B). However, expression levels of *JAZ1* continued to maintain reduced levels and showed 27.2-fold increase in *ANAC042* levels (Figure 5B). While *ANAC042* overexpression or *JAZ1* knockout alone can regulate *WRKY33* and *MYB15*, their combined effect in *p35S::ANAC042 jaz1-1* does not further enhance their expression, indicating regulation of these genes are through a shared pathway.

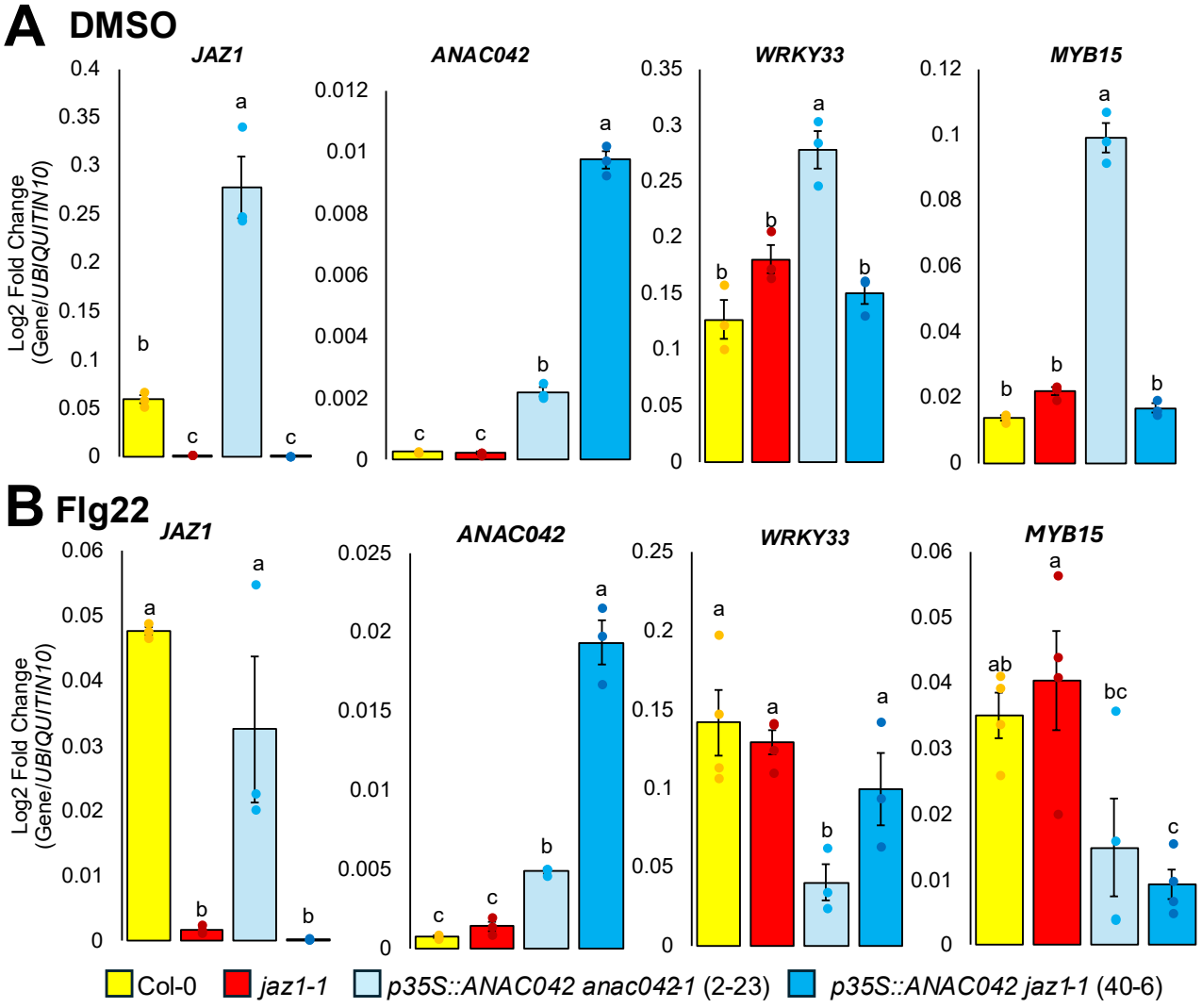

Figure 5. Effects of *ANAC042* overexpression on the expression of other phytoalexins transcription factor genes in wildtype and *jaz1-1* backgrounds. Expression levels of phytoalexin-related transcription factor genes in Col-0, *jaz1-1*, *p35S::ANAC042 anac042-1* (2-23), and *p35S::ANAC042 jaz1-1* (40-6). Arabidopsis seedlings after 10 days of **(A)** DMSO and **(B)** Flg22 treatment and quantified by qRT-PCR. Different letters show significant differences by single factor ANOVA, Tukey post-hoc test, $p < 0.01$, $\alpha = 0.05$. Error bars represent SE, n = three to four per treatment.

3.4 JAZ1 and ANAC042 are involved in regulating growth-defense trade-offs

While the concept of trade-offs between growth and defense have been well-documented, it remains to be determined whether phytoalexin regulators play a role (Campos et al., 2016; Huot et al., 2014; Karasov et al., 2017; Xu et al., 2017). To investigate, we compared the growth-inhibitory effects of the bacterial elicitor, Flg22, on the seedling dry weights of *jaz1-1*, *p35S::ANAC042 anac042-1*, and *p35S::ANAC042 jaz1-1*. Measurements under both conditions revealed genotype specific growth patterns that reflect growth-defense trade-offs. Without elicitation, all genotypes showed weights comparable to wildtype (Figure 6). Following Flg22 treatment, wildtype growth was reduced by 1.8-fold, and as expected, *fls2* showed no growth impairment. The growth of *jaz1-1* was reduced by 2.3-fold, which was insignificant compared to the wildtype. By contrast, *ANAC042* overexpression alleviated Flg22's suppression of growth, however it failed to surpass wildtype levels when combined with the *jaz1-1* mutation (Figure 6). These results demonstrate that JAZ1 and ANAC042 may regulate Flg22-mediated growth suppression through mechanisms that favour growth. .

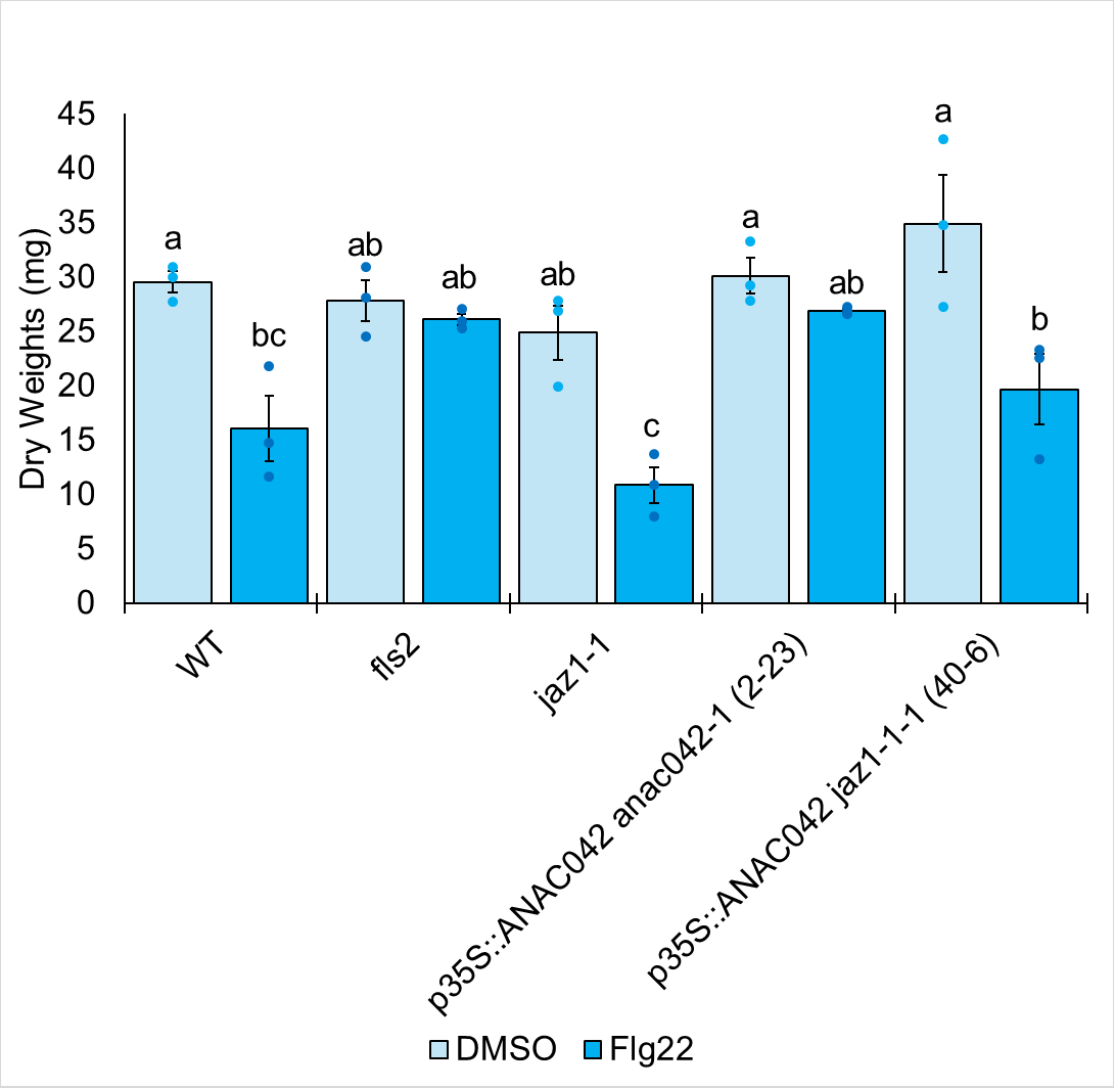

Figure 6. Dry weight measurements of wildtype, *fls2*, *jaz1-1*, *p35S::ANAC042* (2-23), and *p35S::ANAC042 jaz1-1* (40-6) after 10 days of DMSO or Flg22 treatment. Different letters show significant differences by single factor ANOVA, Tukey post-hoc test, $p < 0.01$, $\alpha = 0.05$. Error bars = SE, n = three.

3.5 Main Takeaways

To summarize, our multigene manipulation techniques in Arabidopsis revealed that JAZ1 is responsive to prolonged exposure to Flg22, and that combined with *ANAC042* overexpression with *JAZ1* knockout stimulates substantial 4OH-ICN accumulation without an elicitor. Interestingly, camalexin levels remained low despite both sharing the same precursor, IAOx. In addition, the biosynthetic gene expression patterns of 4OH-ICN did not reflect the amount

observed. Regarding growth-defense trade-offs, *ANAC042* overexpression mitigated growth penalties from Flg22, producing larger seedlings compared to the *jaz1-1* mutant, whose growth was significantly reduced. Thus, in the balance between growth or defense, both ANAC042 and JAZ1 ultimately act to favour growth.

CHAPTER 4: DISCUSSION

4.1 Transcriptional control of adaptation to chronic stress

To contextualize our findings on *p35S::ANAC042 jaz1-1*, it is important to first briefly understand how plants adapt to long-term stress and what is known about specific regulators involved in this process. Under stress, plants divert resources away from growth and focus on defense to maximize survival (Wang et al., 2018). However, chronic or prolonged stress exposure triggers adaptation responses that are distinct from acute, short-term defense. During long-term immune responses, plants will shift resources from rapid immune activation to a more sustainable balance involving hormonal recalibration by limiting JA, salicylic acid (SA), and ET signals, reducing the accumulation of those defense hormones. They also reduce the expression of energy-expensive growth pathways, including cell division and primary metabolism, and upregulate senescence-related processes that reallocate nutrients and energy to provide an intermediate level of defense and growth (Flexas et al., 2006; Gururani et al., 2015). JA plays a vital role in this balancing act between growth and defense in chronic stress. Prolonged JA signaling induces negative feedback by upregulating *JAZ* expression. JAZ proteins in turn suppress TFs such as MYCs to dampen defense gene activation (Chung and Howe, 2009; Howe et al., 2018). Under non-elicited conditions, JAZ1 represses MYC2, preventing the activation of JA-responsive defense genes. In canonical JA signaling, elicitation leads to JA-Ile perception by the Skp1-cullin-F-box $(SCF)^{COI}$ complex, which targets JAZ proteins for proteasomal degradation, releasing MYC2 to activate downstream gene expression (Chini et al., 2007). Beyond this canonical pathway, gibberellin (GA) signaling, responsible for mediating plant development such as shoot elongation and aid in the development of the secondary cell wall, also intersects with JA signaling pathway (Castro-Camba et al., 2022; Hou et al., 2010). DELLA proteins, which accumulate under low GA, bind to JAZ1 to restrain MYC2 inhibition activity, indirectly promoting JA responses (Hou et al., 2010). During this time, DELLAs reduce growth

by sequester phytochrome-interacting factors to prevent the promoting of stem elongation or cell expansion (Hou et al., 2010). This dual action of DELLAs provides an additional layer of regulation during chronic stress as this time is when plants must actively suppress growth while maintain a sustainable level of defense. These adjustments are fundamental for maintaining homeostasis while continuing to defend against persistent threats. To transition from acute responses to long-term adaptation, growth must be actively suppressed to conserve energy, and defense signals must be tightly regulated to prevent self-inflicted damages (Guruani et al., 2015).

In this study, the effects of *ANAC042* overexpression in *jaz1-1* mutant background was investigated to assess the contribution of ANAC042 lacking *JAZ1* influences sustained immune responses. JAZ repressors, including JAZ1, have been shown to play key roles in resetting defense programs after pathogen stress, helping to re-establish growth by silencing stress-responsive genes once a threat subsides (Campos et al., 2016; Guo et al., 2018). Although JAZ proteins are degraded in the presence of JA-Ile to permit JA TF activation, this degradation is transient. JA signaling itself induces the transcription of *JAZ* genes, leading to the replenishment of JAZ proteins that rebind to MYC2 and other TFs, thereby restoring repression after the onset of defense activation (Hou et al., 2010; Guo et al., 2018). In addition, the presence of JA-Ile triggers the degradation of numerous JAZ proteins, but JA-Ile turnover by IAR3 and ILL6 ensures that defense activation is not sustained once stress signals diminish (Widemann et al., 2013). This repressive function is to avoid chronic JA overstimulation, which can become detrimental to plant development if too much is present. Higher-order *jaz* mutants such as *jazQ* and *jazD* exhibit strong growth inhibition and precocious senescence, highlighting the role of JAZ proteins in inhibiting prolonged defense responses (Campos et al., 2016; Guo et al., 2018). Our finding that *jaz1-1* mutant had significantly reduced biomass under prolonged Flg22 exposure aligns with this model of JA repressing defenses and supporting plant growth (Figure 6).

Although ANAC042 is extensively studied for its active role in redox signaling and stress defense, evidence suggests it also contributes to long-term stress adaptation. The loss-of-function mutant *anac042-1* exhibits early onset chlorophyll degradation and accelerated senescence under stress conditions, indicating that ANAC042 functions in promoting organ longevity during prolonged hydrogen peroxide stress (Wu et al., 2012). Our data indicates the overexpression of

ANAC042 alone prevented Flg22-stimulated growth reduction, whereas an exaggerated growth reduction occurred in the *jaz1-1* background (Figure 6). However, the overexpression of *ANAC042* combined with *JAZ1* knockout showed intermediate growth between both single genotypes and had a similar growth to wildtype, suggesting that ANAC042 and JAZ1 have an antagonistic relationship, where both have opposing regulatory effects on growth (Figure 6). It would be worth investigating whether the overexpression of *ANAC042* in backgrounds lacking each of the 13 Arabidopsis *JAZ* genes would provide insight on whether we can unlock phytoalexin biosynthesis without hindering plant growth. In soybean, GmNAC42-1 is bound by GmJAZ1-9 under unelicited conditions and released upon elicitor perception, enabling defense activation (Lin et al., 2025). Taken together, these findings raise the possibility that JAZ1 inhibits ANAC042 to promote growth under non-elicited conditions, while loss of *JAZ1* may relieve this inhibition to allow ANAC042 to activate defense gene expression during stress. Beyond ANAC042 and JAZ1, other TFs orchestrate plant responses to long-term stress exposure. WRKY70, initially identified as a positive regulator of SA-dependent immunity against *Pseudomonas syringae*, also suppresses premature leaf senescence. Loss-of-function *wrky70* mutant develop early chlorophyll breakdown, linking defense activation to delayed aging processes (Li et al., 2004; D. Wang et al., 2006). Similarly, CAMTA3 prevents prolonged immune responses as suggested by the constitutive accumulation of SA, even in the absence of elicitation (Sun et al., 2020). To date, no published studies have demonstrated a direct interaction or coordinated regulatory role between ANAC042 and either WRKY70 or CAMTA3 in the context of delaying senescence. While all three TFs are individually implicated in stress responses and senescence regulation, their functional convergence remain uncharacterized. Future studies will be necessary to determine whether ANAC042 operates independently or as part of a broader regulatory network involving WRKY70 or CAMTA3 during long-term stress adaptation. To determine how the losing the JAZ1 function can affect phytoalexin biosynthesis, the next subsection examines how Flg22-elicited lignin deposition causes derepression when JAZ1 is knocked out.

4.2 Knocking out *JAZ1* derepresses Flg22-elicited lignin deposition

JAZ1 is a key transcriptional repressor in the JA signaling pathway, where it inhibits TFs until its degradation is triggered by JA-Ile through the SCF^{COI1} complex (Chini et al., 2007).

Beyond its role in defense, JAZ1 has been associated with early organ development, as it is rapidly induced within 30 minutes of auxin signaling, and suppresses early stages of lateral root development, also influencing flowering time and reproductive development (Grunewald et al., 2009; Zhai et al., 2015). All members of the *JAZ* family share the core function of repressing JA signaling by interacting with MYC TFs, but JAZ1 acts as a broad-spectrum regulator, interacting with multiple TFs across diverse pathways (Chini et al., 2007; Thines et al., 2007). A distinct role for JAZ1 was recently discovered in soybean. The Arabidopsis *JAZ1* homolog, namely *GmJAZ1*, was unresponsive to short-term (24 h) ABA treatment, but was strongly upregulated after six days of ABA or dehydration treatment. As a result, silencing *GmJAZ1* suppressed glyceollin accumulation at this stage, implicating its role in adapting to chronic stress (Lin et al., 2025). Similarly, here our time-course analysis of Flg22-induced lignification in Arabidopsis revealed that the loss-of-function *jaz1-1* mutant and wildtype exhibited similar lignification patterns after two days. However, by day four, lignification in the wildtype subsided, while it intensified in *jaz1-1*, indicating that JAZ1 suppresses prolonged stress-induced lignification in Arabidopsis. Further supporting JAZ1's function as a long-term suppressor of biochemical defenses, Lin and colleagues reported that silencing *GmJAZ1* led to elevated accumulation of glyceollins under prolonged dehydration and ABA exposure (Lin et al., 2025). Similarly, in Arabidopsis, prolonged cold and salt stress enhanced camalexin accumulation in *jaz1* mutant, linking JAZ1 repression to the regulation of phytoalexins biosynthesis under sustained stress (Makhazen et al., 2021). These results reinforce the role of JAZ1 as a conserved negative regulator of chronic metabolic responses by delaying lignin biosynthesis and other specialized metabolite production. In plants, the synthesis of secondary cell walls are tightly regulated by hierarchical transcriptional networks and comprised of cellulose, hemicellulose, and lignin, with MYB46 serving as a master regulator whose activation is influenced by MYC2 from the JA pathway (Im et al., 2023; Taylor-Teeples et al., 2015; H. Z. Wang and Dixon, 2012). Under non-stress conditions, MYC2 is bound by JAZ1, preventing activation of JA-responsible genes and interaction with *MYB46* promoters (Chini et al., 2007). While it remains unclear whether JAZ1 influences lignin catabolism, current evidence supports a role for JAZ1 in dampening lignin accumulation by interfering with JA signaling and other TF activities. These observations highlight how ANAC042 and JAZ1 act as opposing regulators of long-term stress, which raises the question of how the loss of JAZ1

specifically alters downstream defense outputs. To address this, the next subsection examines how *JAZ1* knockout combined with *ANAC042* overexpression accumulate phytoalexins.

4.3 *JAZ1* knockout combined with *ANAC042* overexpression mediates phytoalexin biosynthesis in Arabidopsis

4.3.1 Knocking out *JAZ1* and simultaneously overexpressing *ANAC042* causes massive 4OH-ICN and monolignol accumulation

Our data demonstrated that simultaneous overexpression of *ANAC042* in the absence of *JAZ1* led to a selective increase in phytoalexin metabolism, particularly the Trp-derived 4OH-ICN and Phe-derived monolignols H, G, and S. Notably, 4OH-ICN accumulation was strongly induced and surpassed wildtype levels under both conditions (Figure 4A). These results indicate that multigene manipulation is a successful strategy for unlocking the chronic production of select phytoalexin metabolites.

A recent study conducted in soybean found that GmJAZ1 negatively regulates the activity of GmNAC42-1, and silencing *GmJAZ1* relieves this repression to enable glyceollin accumulation in the presence of stress (Lin et al., 2025). In Arabidopsis, knocking out *JAZ1* in combination with overexpressing *ANAC042* exhibited greater accumulation of 4OH-ICN than either single genotype alone. Additionally, in the *p35S::ANAC042 anac042-1* background, *ANAC042* overexpression rescued the reduced expression of *CYP71A12* and *FOX1* of the *anac042-1* mutant, while also upregulating *CYP82C2* levels (Figure 4D). However, at an earlier time point (12 hours), *p35S::ANAC042 anac042-1* Arabidopsis seedlings showed 4OH-ICN levels comparable to wildtype and a significantly reduced *CYP82C2* expression in *anac042-1* mutants, suggesting that ANAC042 is involved in the regulation of 4OH-ICN, but *ANAC042* overexpression alone is insufficient to elevate 4OH-ICN beyond wildtype levels during the acute stress responses (Monsalvo et al., 2025). Collectively, these results suggest that either process regulated by ANAC042 or JAZ1 alone is insufficient to unlock phytoalexin biosynthesis, yet their combination enhances the production of select phytoalexins.

ANAC042 has been recognized as a key regulator of Trp-derived phytoalexins, particularly camalexin and 4OH-ICN (Saga et al., 2012). Recent evidence has expanded this view, linking ANAC042 to the regulation of Phe-derived phytoalexins as well, a pathway

historically controlled by MYB TFs such as MYB15 (Chezam et al., 2017). *ANAC042* overexpression increased *PAL* expression, but reduced in *anac042-1* mutants. Although monolignol and scopoletin accumulation did not excel wildtype levels, *ANAC042* overexpression lines exhibited systemic lignification upon Flg22 elicitation, while *anac042-1* failed to lignify (Monsalvo et al., 2025). These findings reinforce ANAC042's broader role in activating lignin biosynthesis during defense responses and correlate to what was observed in our data, where *PAL* expression was highest in *p35S::ANAC042 jaz1-1* and *p35S::ANAC042 anac042-1* showed moderate to similar expression to wildtype, respectively. A similar trend was observed with monolignol accumulation under Flg22 treatment, where only *p35S::ANAC042 jaz1-1* produced detectable amounts of monolignol H, G, and S, while other genotypes did not (Figure 4B). Although lignin staining showed some stem lignification across all genotypes under mock conditions, only *p35S::ANAC042 jaz1-1* exhibited both monolignol accumulation and systemic lignin deposition in response to Flg22 (Figure 4B and 4E). These results further reinforce that simultaneous overexpression of *ANAC042* and knockout of *JAZ1* is required to activate these phytoalexin pathways. Dual manipulation revealed an unexpected selectivity in which phytoalexins are to accumulate. In this case, 4OH-ICN and several monolignols were strongly accumulated. This motivates a closer investigation of whether transient regulation may explain the restriction accumulation of other metabolites.

4.3.2 Transient regulation limits phytoalexin accumulation and is deregulated by *p35S::ANAC042 jaz1-1*

Despite the strong elicitation of 4OH-ICN and monolignols in *p35S::ANAC042 jaz1-1*, camalexin, scopoletin, and few other monolignol derivatives remained undetectable, highlighting the selective nature of this metabolic reprogramming (Figure 4A and 4B). A recent study demonstrated that ANAC042 activates camalexin biosynthesis within a day of Flg22 elicitation. However, camalexin fails to accumulate after 10 days post-elicitation, a time point when JAZ1-mediated repression is active. *p35S::ANAC042 jaz1-1* failed to surpass wildtype levels, despite exhibiting elevated expression of camalexin synthesis gene *CYP71B15*, suggesting that a shortage of substrate may restrict camalexin biosynthesis (Figure 4A and 4D). However, a deeper investigation into the substrate levels for 4OH-ICN and camalexin revealed abundant accumulation of IAOx, dismissing the possibility of a substrate bottleneck (Figure 4A). While monolignols H and G were strongly induced, monolignol derivatives 5H and C, along with

scopoletin, were not detected (Figure 4B). Interestingly, their precursor, caffeic acid, accumulated in high amounts (Figure 4B). The differential accumulation of metabolites in response to *ANAC042* overexpression combined with *JAZ1* knockout may reflect differences in cellular and tissue localization of these phytoalexins. To better understand why certain metabolites like 4OH-ICN and some monolignols accumulate while others do not, it is important to consider their localization to gain insights on phytoalexin secretion and retention. Monolignol biosynthesis predominately occurs in the cytosol, and the synthesized compounds are then transported to the apoplast, where they form lignin in the cell wall through oxidative polymerization (Liu et al., 2018; Meents et al., 2018). On the other hand, camalexin production is tightly localized to wound sites during infection. Its biosynthesis involves cytochrome P450 enzymes, such as *CYP71A13* and *CYP71B15*, which are embedded in the endoplasmic reticulum (Mucha et al., 2019). These P450 enzymes reorganize to interact with other enzymes on organelles or with additional P450 enzymes (Fuchs et al., 2016). While there is currently no direct evidence for the localization of 4OH-ICN, it may follow a similar pattern to camalexin, given that both pathways involve cytochrome P450 enzymes anchored to the endoplasmic reticulum (Bak et al., 2011; Reed and Backes, 2012). Another possible explanation for high 4OH-ICN and low camalexin levels may be related to transport. Camalexin export relies on specific plasma membrane ABCG transporters such as PEN3 and PDR12, which secrete camalexin into the apoplast during infection. Loss-of-function mutations in these transporters result in intracellular camalexin accumulation, indicating a failure in secretion (He et al., 2019). It is possible that JAZ1 may play a role in camalexin transport, and its repression may lead to intracellular accumulation of camalexin, although this remains unknown.

Another explanation for the observed discrepancy, where 4OH-ICN levels were elevated while camalexin and other phytoalexins remained low, is that the expression of certain genes and the accumulation of their associated metabolites may be transient, rendering them difficult to detect at steady state. For instance, *JAZ1* transcript levels in *wrky33* mutants were reported to increase progressively over a 48 hour period, whereas expression in Col-0 exhibited only transient peaks. Likewise, *CYP71A12* expression was shown to be transient in both *anac042* mutants and Col-0 following elicitation (Saga et al., 2012). These observations highlight the importance of precise timing of transcriptional activation, and that single time-point analysis may fail to capture transient or tightly regulated defense responses. The next section explores

how ANAC042 and JAZ1 interact within a broader transcriptional network governing immune response.

4.4 Network manipulation- regulating phytoalexin biosynthesis by overexpressing *ANAC042* and knocking out *JAZ1*

Investigating *ANAC042* overexpression and *JAZ1* knockout uncovers how these two factors modulate phytoalexin biosynthesis through a broader protein regulatory network. It was previously reported that *WRKY33* transcript levels remain unchanged in *ANAC042* knockout and overexpression lines following short-term Flg22 elicitation (Saga et al., 2012; Monsalvo et al., 2025). However, ANAC042 can bind to promoters of *CYP71A13* and *CYP71B15*, which are also direct targets of WRKY33 (Monsalvo et al., 2025; Saga et al., 2012; Zheng et al., 2006).Our long-term Flg22 data showed that *ANAC042* overexpression alone significantly downregulated *WRKY33* expression, and this downregulation was only partially alleviated in *jaz1-1* mutant (Figure 5B). These results support the idea that ANAC042 does not directly regulate *WRKY33* expression under immune stress, but instead relies on JAZ1 to partially suppress *WRKY33* expression during later stages of elicitation.

Similarly, *MYB15* has been implicated in regulating Phe-derived phytoalexins, and recent work suggests it may also be a downstream target of ANAC042. In the absence of *ANAC042*, *MYB15* expression levels were significantly reduced, whereas overexpression of *ANAC042* in the *anac042-1* background partially restored *MYB15* expression to wildtype levels (Monsalvo et al., 2025). However, *MYB15* appeared to be downregulated by ANAC042 alone under long-term stress, as seen by its reduced expression in overexpression lines. While *jaz1-1* mutant retained wildtype levels of *MYB15*, combining this mutant with *ANAC042* overexpression caused a significant reduction in *MYB15* levels (Figure 5B). This suggests that ANAC042 may play a dual role in *MYB15* regulation by activating its expression during early immune responses and potentially contributing to its downregulation at later stages to prevent overaccumulation or saturation effects in prolonged stress.

Transcript analysis further revealed that *ANAC042* expression remained low in both wildtype and *jaz1-1* backgrounds, but were strongly elevated in *p35S::ANAC042 anac042-1* and *p35S::ANAC042 jaz1-1* genotypes (Figure 5A and 5B). This indicates that loss of *JAZ1* alone

does not manipulate *ANAC042* transcription, indicating that JAZ1 is unlikely to act as a direct transcriptional repressor of ANAC042 at a later stage. Instead, the elevated *ANAC042* expression levels were observed only in transgenic lines driven by the CaMV *35S* promoter, proposing that the elicitation was due to transgene activity opposed to endogenous repression relief (Odell et al., 1985). These findings of contrasting genotypes provided a distinct framework on how ANAC042 accumulation modulates downstream immune responses and phytoalexin biosynthesis.

JAZ1 expression levels remained consistently low in both *jaz1-1* and *p35S::ANAC042 jaz1-1* lines regardless of Flg22 treatment, validating the effectiveness of the *JAZ1* knockout. In wildtype plants, *JAZ1* levels was significantly high under mock treatment, but declined following Flg22 exposure, consistent with previous reports that *JAZ* genes are induced early during immune responses and later repressed to restore homeostasis in JA signaling (Figure 5B; Chini et al., 2007). In *p35S::ANAC042 anac042-1*, *JAZ1* levels were already extremely high under non-elicited conditions and remained elevated upon Flg22 elicitation, though to a slightly lesser degree than wildtype (Figure 5B). This suggests that constitutive *ANAC042* overexpression may activate JA-responsive genes, including *JAZ1*, even in the absence of elicitation, potentially through indirect modulation of JA-related TFs. Overall, these results suggest that *JAZ1* is a highly Flg22-responsive gene whose transcription can also be regulated by ANAC042. The data also supports that JAZ1 may be a point of convergence between multiple signaling pathways, functioning as a negative feedback regulator. This cooperative regulation among different players provides insights into how manipulating ANAC042 and JAZ1 shapes this network, but it also reveals gaps in our current mechanistic understanding. Building on this framework, the following subsection outlines key limitations and future experimental directions that are necessary to address these unknowns.

4.5 Limitations and Future Directions

While our findings support the hypothesis that knocking out *JAZ1* derepresses phytoalexin biosynthesis, and that combining it with *ANAC042* overexpression further enhances defense metabolite accumulation, several limitations constrain the full interpretation of these results and point to valuable avenues for future investigations.

Although we observed strong systemic lignification and high accumulation of 4OH-ICN in the line that overexpresses *ANAC042* lacking *JAZ1*, these changes occurred without significant upregulation of lignin or 4OH-ICN biosynthetic genes (Figure 4A-C). Phytoalexins are often induced and then metabolized after stress subsides as plants divert resources back to growth (He et al., 2022; Huot et al., 2014; Karasov et al., 2017). For example, phytoalexins such as camalexin peak shortly after elicitation (18-24 hours) and decline after (Saga et al., 2012). This phytoalexin degradation behaviour parallels findings in soybean, where silver nitrate ($AgNO_3$) indirectly prevented the degradation of glyceollin I production by promoting the hydrolysis of its isoflavone conjugate, 6″-*O*-malonyldaidzin to increase daidzein precursor availability for glyceollin biosynthesis (Farrell et al., 2017; Yoshikawa, 1978). In contrast, bacterial elicitors like WGE significantly solely increased glyceollin amounts without affecting its degradation (Yoshikawa, 1978). Meanwhile, phytoalexin compounds are often secreted into the extracellular space or culture medium, where they encounter high peroxidase activities capable of degrading phenolic compounds such as glyceollin or medicarpin (Barz et al., 1990). These considerations may explain the high 4OH-ICN and relatively low camalexin and scopoletin in *p35S::ANAC042 jaz1-1*, which may impair catabolic enzyme activities for 4OH-ICN turnover. However, the lack of transcriptomic profiling limits our ability to identify differentially expressed catabolic genes. Future studies using RNA-seq analysis could help uncover candidates and determine whether ANAC042-mediated regulation or *JAZ1* knockout alters their expression, offering insight into the regulation of phytoalexin catabolism.

A second limitation concerns the reliance on a single post-elicitation time point, which offers only a snapshot of a highly dynamic defense response. Many phytoalexins are transiently induced following PAMP perception (Rajniak et al., 2015). For example, camalexin and scopoletin tends to peak within 12-48 hours post-elicitation before rapidly declining (Beyer et al., 2019; Saga et al., 2012). The low abundance of certain metabolites in *p35S::ANAC042 jaz1-1* may potentially reflect timing effects rather than an inability to accumulate them. Additionally, although *p35S::ANAC042 jaz1-1* is driven by the constitutive *35S* promoter, other defense-associated TFs may exhibit cyclic activation that are influenced by circadian and seasonal rhythms (Román et al., 2021; Silva et al., 2020). Without a time-course experiment, we cannot distinguish whether transient activation was missed or if delayed elicitation occurred between elicitation and harvest. Analyzing these time-course studies would enable us to determine the

onset, peak, and decline phases for each metabolite, and reveal how *ANAC042* overexpression and *JAZ1* knockout influences these defense activations.

Third, while our study examined *ANAC042* overexpression in a *JAZ1*-deficient background, we did not assess whether pairing it with other TFs could broaden defense outputs. Both WRKY33 and ANAC042 can directly activate *CYP71A13* and *CYP71B15* in the camalexin pathway, and both are implicated in regulating 4OH-ICN accumulation (Barco et al., 2019; Birkenbihl et al., 2012; Monsalvo et al., 2025). Given that *p35S::ANAC042 jaz1-1* showed strong 4OH-ICN, but minimal camalexin accumulation, the co-overexpression of *WRKY33* and *ANAC042* in a *JAZ*-deficient line could test whether simultaneous activation of multiple phytoalexin pathways could achieve higher yields. Such an approach could help determine whether the selective metabolite profiles we observed arise from regulatory bottlenecks at the TF level or from constraints in enzyme activity, such as low enzymatic activity or inhibition of enzymes that we are unaware of.

Lastly, this study advances current understanding of JAZ-NAC interactions in defense reprogramming, but also highlights the importance of moving beyond single-factor manipulations. Many TFs operate cooperatively within regulatory networks and overcoming JA repression appears to be a prerequisite for broad phytoalexin activation in Arabidopsis. Testing whether this principle applies to legumes could reveal its broader relevance. For example, it was demonstrated that multigene stacking using a P2A peptide linker can achieve high yields of target metabolites in other plant hosts, such as tobacco and Arabidopsis (Liao et al., 2022). Inspired by this strategy, we propose linking *GmHSF6-1* and *GmMYB29A2* with a P2A linker in a constitutive expression vector that contains *GmJAZ1-9* RNAi to test whether glyceollins and other phytoalexin levels can be similarly enhanced (Figure 7). This cross-species approach could shed light on whether the immune activation observed in Arabidopsis can be extended to other plant species, such as soybean.

4.6 Significance

Investigating the consequences of multigene manipulation on phytoalexin production could provide novel insights and substantially advance our understanding of phytoalexin pathway elicitation. TFs often function cooperatively within complex regulatory networks,

integrating multiple signaling cues to balance growth and defense responses (De Bruyne et al., 2014; Huot et al., 2014). Dissecting which TF combinations most effectively unlock phytoalexin biosynthesis may reveal synergistic defense activation that single-gene manipulation fail to capture. Extending these findings beyond Arabidopsis, identifying key combinatorial regulators could enable targeted elicitation of phytoalexins in diverse plant species, offering valuable opportunities for pharmaceutical applications and the engineering of high-value defense metabolites in non-native hosts (Jeandet et al., 2014).

4.7 Conclusion

This study demonstrates that knocking out *JAZ1* derepresses phytoalexin biosynthesis in Arabidopsis and its combination with *ANAC042* overexpression significantly enhances the accumulation of key defense metabolites like 4OH-ICN. Also, *jaz1-1* loss-of-function accelerates systemic lignification and impacts TFs under non-elicited conditions. Loss of *JAZ1* also intensifies growth suppression under stress, signifying growth-defense trade-offs. The development of a dual-gene plasmid for glyceollin biosynthesis in soybean provides a promising tool to translate these findings into other plant species. Overall, our results emphasize the need for multigene manipulation to effectively enhance plant immunity and phytoalexin production.

REFERENCES

Alonso, J. M., Stepanova, A. N., Solano, R., Wisman, E., Ferrari, S., Ausubel, F. M., Ecker, J. R. (2003). Five components of the ethylene-response pathway identified in a screen for weak ethylene-insensitive mutants in Arabidopsis. *Proceedings of the National Academy of Sciences of the United States of America*, *100*(5): 2992-2997.

Anderson, J. P., Badruzsaufari, E., Schenk, P. M., Manners, J. M., Desmond, O. J., Ehlert, C., Maclean, D. J., Ebert, P. R., Kazan, K. (2004). Antagonistic interaction between abscisic acid and jasmonate-ethylene signaling pathways modulates defense gene expression and disease resistance in arabidopsis. *Plant Cell*, *16*(12): 3460-3479.

Antika, L. D., Tasfiyati, A. N., Hikmat, H., Septama, A. W. (2022). Scopoletin: A review of its source, biosynthesis, methods of extraction, and pharmacological activities. *Zeitschrift fur Naturforschung - Section C Journal of Biosciences*, *77*(7–8): 303-316.

Bai, Y., Meng, Y., Huang, D., Qi, Y., Chen, M. (2011). Origin and evolutionary analysis of the plant-specific TIFY transcription factor family. *Genomics*, *98*(2): 128-136.

Bak, S., Beisson, F., Bishop, G., Hamberger, B., Höfer, R., Paquette, S., Werck-Reichhart, D. (2011). Cytochromes P450. *The Arabidopsis Book*, *9*: 1-56.

Barco, B., Kim, Y., Clay, N. K. (2019). Expansion of a core regulon by transposable elements promotes Arabidopsis chemical diversity and pathogen defense. *Nature Communications*, *10*(1): 3444.

Barz, W., Bless, W., Borger-Papendorf, G., Gunia, W., Mackenbrock, U., Meier, D., Otto, C. H., Super, E. (1990). Phytoalexins as part of induced defence reactions in plants: their elicitation, function and metabolism. *Ciba Foundation*, *154*: 140-156.

Beyer, S. F., Beesley, A., Rohmann, P. F. W., Schultheiss, H., Conrath, U., Langenbach, C. J. G. (2019). The Arabidopsis non-host defence-associated coumarin scopoletin protects soybean from Asian soybean rust. *Plant Journal*, *99*(3): 397-413.

Birkenbihl, R. P., Diezel, C., Somssich, I. E. (2012). Arabidopsis WRKY33 is a key transcriptional regulator of hormonal and metabolic responses toward Botrytis cinerea infection. *Plant Physiology*, *159*(1): 266-285.

Boerjan, W., Ralph, J., Baucher, M. (2003). Lignin Biosynthesis. *Annual Review of Plant Biology*, *54:* 519–546.

Campos, M. L., Yoshida, Y., Major, I. T., De Oliveira Ferreira, D., Weraduwage, S. M., Froehlich, J. E., Johnson, B. F., Kramer, D. M., Jander, G., Sharkey, T. D., Howe, G. A. (2016). Rewiring of jasmonate and phytochrome B signalling uncouples plant growth-defense tradeoffs. *Nature Communications*, *7*: 1-10.

Castro-Camba, R., Sánchez, C., Vidal, N., Vielba, J. M. (2022). Plant Development and Crop Yield: The Role of Gibberellins. *Plants*, *11*(19): 2650.

Chao, Q., Rothenberg, M., Solano, R., Roman, G., Terzaghi, W., Ecker, J. R. (1997). Activation of the ethylene gas response pathway in Arabidopsis by the nuclear protein ETHYLENE-INSENSITIVE3 and related proteins. *Cell*, *89*(7): 1133-1144.

Chen, Q., Wang, Q., Xiong, L., Lou, Z. (2011). A structural view of the conserved domain of rice stress-responsive NAC1. *Protein and Cell*, *2*(1): 55–63.

Chezem, W. R., Memon, A., Li, F. S., Weng, J. K., Clay, N. K. (2017). SG2-type R2R3-MYB transcription factor MYB15 controls defense-induced lignification and basal immunity in arabidopsis. *Plant Cell*, *29*(8): 1907-1926.

Chinchilla, D., Bauer, Z., Regenass, M., Boller, T., Felix, G. (2006). The Arabidopsis receptor kinase FLS2 binds flg22 and determines the specificity of flagellin perception. *Plant Cell*, *18*(2): 465-476.

Chini, A., Fonseca, S., Fernández, G., Adie, B., Chico, J. M., Lorenzo, O., García-Casado, G., López-Vidriero, I., Lozano, F. M., Ponce, M. R., Micol, J. L., Solano, R. (2007). The JAZ family of repressors is the missing link in jasmonate signalling. *Nature*, *448*(7154): 666-671.

Chung, H. S., Howe, G. A. (2009). A critical role for the TIFY motif in repression of jasmonate signaling by a stabilized splice variant of the JASMONATE ZIM-domain protein JAZ10 in Arabidopsis. *Plant Cell*, *21*(1): 131-145.

Clough, S. J., Bent, A. F. (1998). Floral dip: A simplified method for Agrobacterium-mediated transformation of Arabidopsis thaliana. *Plant Journal*, *16*(6): 735-743.

Demidchik, V., Nichols, C., Oliynyk, M., Dark, A., Glover, B. J., Davies, J. M. (2003). Is ATP a Signaling Agent in Plants? *Plant Physiology*, *133*(2): 456-461.

Denoux, C., Galletti, R., Mammarella, N., Gopalan, S., Werck, D., De Lorenzo, G., Ferrari, S., Ausubel, F. M., Dewdney, J. (2008). Activation of defense response pathways by Ogs and Flg22 elicitors in Arabidopsis seedlings. *Molecular Plant*, *1*(3): 423-445.

Farrell, K., Jahan, M. A., Kovinich, N. (2017). Distinct mechanisms of biotic and chemical elicitors enable additive elicitation of the anticancer phytoalexin glyceollin I. *Molecules*, *22*(8): 1261.

Flexas, J., Bota, J., Galmés, J., Medrano, H., Ribas-Carbó, M. (2006). Keeping a positive carbon balance under adverse conditions: Responses of photosynthesis and respiration to water stress. *Physiologia Plantarum*, *127*(3): 343-352.

Fuchs, R., Kopischke, M., Klapprodt, C., Hause, G., Meyer, A. J., Schwarzländer, M., Fricker, M. D., Lipka, V. (2016). Immobilized subpopulations of leaf epidermal mitochondria mediate PENETRATION2-dependent pathogen entry control in arabidopsis. *Plant Cell*, *28*(1): 130-145.

Grunewald, W., Vanholme, B., Pauwels, L., Plovie, E., Inzé, D., Gheysen, G., Goossens, A. (2009). Expression of the Arabidopsis jasmonate signalling repressor JAZ1/TIFY10A is stimulated by auxin. *EMBO Reports*, *10*(8): 923-928.

Guo, Q., Yoshida, Y., Major, I. T., Wang, K., Sugimoto, K., Kapali, G., Havko, N. E., Benning, C., Howe, G. A. (2018). JAZ repressors of metabolic defense promote growth and reproductive fitness in Arabidopsis. *Proceedings of the National Academy of Sciences of the United States of America*, *115*(45): 1-10.

Gururani, M. A., Venkatesh, J., Tran, L. S. P. (2015). Regulation of photosynthesis during abiotic stress-induced photoinhibition. *Molecular Plant*, *8*(9): 1304-1320.

He, Y., Xu, J., Wang, X., He, X., Wang, Y., Zhou, J., Zhang, S., Meng, X. (2019). The arabidopsis pleiotropic drug resistance transporters PEN3 and PDR12 mediate camalexin secretion for resistance to botrytis cinerea. *Plant Cell*, *31*(9): 2206-2222.

He, Z., Webster, S., He, S. Y. (2022). Growth–defense trade-offs in plants. *Current Biology*, *32*(12): 634-639.

Hilgarth, R. S., Lanigan, T. M. (2020). Optimization of overlap extension PCR for efficient transgene construction. *MethodsX*, *7*: 1-8.

Hou, X., Lee, L. Y. C., Xia, K., Yan, Y., Yu, H. (2010). DELLAs Modulate Jasmonate Signaling via Competitive Binding to JAZs. *Developmental Cell*, *19*(6): 884-894.

Howe, G. A., Major, I. T., Koo, A. J. (2018). Modularity in Jasmonate Signaling for Multistress Resilience. *Annual Review of Plant Biology, 55*(23): 387-415.

Hu, P., Zhou, W., Cheng, Z., Fan, M., Wang, L., Xie, D. (2013). JAV1 Controls Jasmonate-Regulated Plant Defense. *Molecular Cell*, *50*(4): 504-515.

Huang, X. Q., Dudareva, N. (2023). Plant specialized metabolism. *Current Biology*, *33*(11).

Huot, B., Yao, J., Montgomery, B. L., He, S. Y. (2014). Growth-defense tradeoffs in plants: A balancing act to optimize fitness. *Molecular Plant*, *7*(8): 473-478.

Im, J. H., Son, S., Kim, W. C., Kim, K., Mitsuda, N., Ko, J. H., Han, K. H. (2023). *Jasmonate activates secondary cell wall biosynthesis through MYC2-MYB46 module*, *117*: 1099-1114.

Jahan, M. A., Harris, B., Lowery, M., Coburn, K., Infante, A. M., Percifield, R. J., Ammer, A. G., Kovinich, N. (2019). The NAC family transcription factor GmNAC42-1 regulates biosynthesis of the anticancer and neuroprotective glyceollins in soybean. *BMC Genomics*, *20*(1): 149.

Jahan, M. A., Harris, B., Lowery, M., Infante, A. M., Percifield, R. J., Kovinich, N. (2020). Glyceollin transcription factor GmMYB29A2 regulates soybean resistance to phytophthora sojae. *Plant Physiology*, *183*(2): 530-546.

Jeandet, P., Hébrard, C., Deville, M. A., Cordelier, S., Dorey, S., Aziz, A., Crouzet, J. (2014). Deciphering the role of phytoalexins in plant-microorganism interactions and human health. *Molecules*, *19*(11): 18033-18056.

Kalli, S., Araya-Cloutier, C., Lin, Y., de Bruijn, W. J. C., Chapman, J., Vincken, J. P. (2020). Enhanced biosynthesis of the natural antimicrobial glyceollins in soybean seedlings by priming and elicitation. *Food Chemistry*, *317*: 126389.

Karasov, T. L., Chae, E., Herman, J. J., Bergelson, J. (2017). Mechanisms to mitigate the trade-off between growth and defense. *Plant Cell*, *29*(4): 666-680.

Koo, A. J. K., Howe, G. A. (2009). The wound hormone jasmonate. *Phytochemistry*, *70*(13-14): 1571-1580.

Le Roy, J., Huss, B., Creach, A., Hawkins, S., Neutelings, G. (2016). Glycosylation is a major regulator of phenylpropanoid availability and biological activity in plants. *Frontiers in Plant Science*, *7*: 735.

Lecomte, S., Chalmel, F., Ferriere, F., Percevault, F., Plu, N., Saligaut, C., Surel, C., Lelong, M., Efstathiou, T., Pakdel, F. (2017). Glyceollins trigger anti-proliferative effects through estradiol-dependent and independent pathways in breast cancer cells. *Cell Communication and Signaling*, *15*(1): 26.

Li, J., Brader, G., Palva, E. T. (2004). The WRKY70 Transcription Factor: A Node of Convergence for Jasmonate-Mediated and Salicylate-Mediated Signals in Plant Defense. *Plant Cell*, *16*(2): 319-331.

Liao, J., Liu, T., Xie, L., Mo, C., Huang, X., Cui, S., Jia, X., Lan, F., Luo, Z., Ma, X. (2022). Plant Metabolic Engineering by Multigene Stacking: Synthesis of Diverse Mogrosides. *International Journal of Molecular Sciences*, *23*(18): 10422.

Lin, J., Monsalvo, I., Jahan, M. A., Ly, M., Wi, D., Martirosyan, I., Jahan, I., Kovinich, N. (2025). ABA-regulated JAZ1 suppresses phytoalexin biosynthesis by binding GmNAC42-1 in soybean. *Current Plant Biology*, *42*: 100453.

Lin, J., Monsalvo, I., Ly, M., Jahan, M. A., Wi, D., Martirosyan, I., Kovinich, N. (2023). RNA-Seq Dissects Incomplete Activation of Phytoalexin Biosynthesis by the Soybean Transcription Factors GmMYB29A2 and GmNAC42-1. *Plants*, *12*(3): 545.

Liu, Q., Luo, L., Zheng, L. (2018). Lignins: Biosynthesis and biological functions in plants. *International Journal of Molecular Sciences*, *19*(2): 335.

Liu, S., Guan, Y., Weng, Y., Liao, B., Tong, L., Hao, Z., Chen, J., Shi, J., Cheng, T. (2023). Genome-wide identification of the NAC gene family and its functional analysis in Liriodendron. *BMC Plant Biology*, *23*(1): 415.

Major, I. T., Guo, Q., Zhai, J., Kapali, G., Kramer, D. M., Howe, G. A. (2020). A phytochrome B-independent pathway restricts at high levels of jasmonate defense. *Plant Physiology*, *183*(2): 733-749.

Makhazen, D. S., Veremeichik, G. N., Shkryl, Y. N., Tchernoded, G. K., Grigorchuk, V. P., Bulgakov, V. P. (2021). Inhibition of the JAZ1 gene causes activation of camalexin biosynthesis in Arabidopsis callus cultures. *Journal of Biotechnology*, *342*: 102-113.

Mao, G., Meng, X., Liu, Y., Zheng, Z., Chen, Z., Zhang, S. (2011). Phosphorylation of a WRKY transcription factor by two pathogen-responsive MAPKs drives phytoalexin biosynthesis in Arabidopsis. *Plant Cell*, *23*(4): 1639-1653.

Marcec, M. J., Tanaka, K. (2022). Crosstalk between calcium and ros signaling during flg22-triggered immune response in arabidopsis leaves. *Plants*, *11*(1): 14.

Martim, D. B., Brilhante, A. J. V. C., Lima, A. R., Paixão, D. A. A., Martins-Junior, J., Kashiwagi, F. M., Wolf, L. D., Costa, M. S., Menezes, F. F., Prata, R., Gazolla, M. C., Aricetti, J. A., Persinoti, G. F., Rocha, G. J. M., Giuseppe, P. O. (2024). Resolving the metabolism of monolignols and other lignin-related aromatic compounds in Xanthomonas citri. *Nature Communications*, *15*(1): 1-17.

Meents, M. J., Watanabe, Y., Samuels, A. L. (2018). The cell biology of secondary cell wall biosynthesis. *Annals of Botany*, *121*(6): 1107-1125.

Memelink, J. (2009). Regulation of gene expression by jasmonate hormones. *Phytochemistry*, *70*(13-14): 1560-1570.

Miedes, E., Vanholme, R., Boerjan, W., Molina, A. (2014). The role of the secondary cell wall in plant resistance to pathogens. *Frontiers in Plant Science*, *5*.

Miki, D., Shimamoto, K. (2004). Simple RNAi vectors for stable and transient suppression of gene function in rice. *Plant Cell Physiology*, *45*(4): 490-495.

Mine, A., Nobori, T., Salazar-Rondon, M. C., Winkelmüller, T. M., Anver, S., Becker, D., Tsuda, K. (2017). An incoherent feed-forward loop mediates robustness and tunability in a plant immune network. *EMBO Reports*, *18*(3): 464-476.

Mohr, P. G., Cahill, D. M. (2003). Abscisic acid influences the susceptibility of Arabidopsis thaliana to Pseudomonas syringae pv. tomato and Peronospora parasitica. *Functional Plant Biology*, *30*(4): 461-469.

Moreno, J. E., Tao, Y., Chory, J., Ballare, C. L. (2009). Ecological modulation of plant defense via phytochrome control of jasmonate sensitivity. *Proceedings of the National Academy of Sciences of the United States of America*, *106*(12): 4935-4940.

Monsalvo, I., Lin, J., Kovinich, N. (2024). Phytoalexin gene regulation in Arabidopsis thaliana – On the verge of a paradigm shift? *Current Plant Biology*, *39*: 100367.

Monsalvo, I., Parasecolo, L., Pullano, S., Lin, J., Shahabi, A., Ly, M., Kwon, H., Mathur, K., Rodrillo, K. A. M., Ifa, D. R., Kovinich, N. (2025). ANAC042 Regulates the Biosynthesis of Conserved- and Lineage-Specific Phytoalexins in Arabidopsis. *International Journal of Molecular Sciences*, *26*(8): 3683.

Mucha, S., Heinzlmeir, S., Kriechbaumer, V., Strickland, B., Kirchhelle, C., Choudhary, M., Kowalski, N., Eichmann, R., Hückelhoven, R., Grill, E., Kuster, B., Glawischnig, E. (2019). The Formation of a Camalexin Biosynthetic Metabolon. *The Plant Cell*, *31*(11): 2697–2710.

Nguyen, N. H., Trotel-Aziz, P., Clément, C., Jeandet, P., Baillieul, F., Aziz, A. (2022). Camalexin accumulation as a component of plant immunity during interactions with pathogens and beneficial microbes. *Planta, 255*(6): 116.

Odell, J. T., Nagy, F., Chua, N. H. (1985). Identification of DNA sequences required for activity of the cauliflower mosaic virus 35S promoter. *Nature*, *313*(6005): 810-812.

Ouaked, F., Rozhon, W., Lecourieux, D., Hirt, H. (2003). A MAPK pathway mediates ethylene signaling in plants. *EMBO Journal*, *22*(6): 1282-1288.

Parasecolo, L., Monsalvo, I. M., Kovinich, N., Ifa, D. R. (2025). Development of a Matrix-Assisted Laser Desorption Ionization High Resolution Mass Spectrometry Method for the Quantification of Camalexin and Scopoletin in Arabidopsis thaliana. *Rapid Communications in Mass Spectrometry*, *39*(6): 9973.

Pauwels, L., Barbero, G. F., Geerinck, J., Tilleman, S., Grunewald, W., Pérez, A. C., Chico, J. M., Bossche, R. Vanden, Sewell, J., Gil, E., García-Casado, G., Witters, E., Inzé, D., Long, J. A., De Jaeger, G., Solano, R., Goossens, A. (2010). NINJA connects the co-repressor TOPLESS to jasmonate signalling. *Nature*, *464*(7289): 788-791.

Pauwels, L., Goossens, A. (2011). The JAZ proteins: A crucial interface in the jasmonate signaling cascade. *Plant Cell*, *23*(9): 3089-3100.

Perkins, M. L., Schuetz, M., Unda, F., Chen, K. T., Bally, M. B., Kulkarni, J. A., Yan, Y., Pico, J., Castellarin, S. D., Mansfield, S. D., Samuels, A. L. (2022). Monolignol export by diffusion down a polymerization-induced concentration gradient. *Plant Cell*, *34*(5): 2080-2095.

Rajniak, J., Barco, B., Clay, N. K., Sattely, E. S. (2015). A new cyanogenic metabolite in Arabidopsis required for inducible pathogen defence. *Nature*, *525*(7569): 376-379.

Reed, J. R., Backes, W. L. (2012). Formation of P450 • P450 complexes and their effect on P450 function. In *Pharmacology and Therapeutics*, *133*(3): 299-310.

Román, Á., Li, X., Deng, D., Davey, J. W., James, S., Graham, I. A., Haydon, M. J. (2021). Superoxide is promoted by sucrose and affects amplitude of circadian rhythms in the evening. *Proceedings of the National Academy of Sciences of the United States of America*, *118*(10): 1-7.

Saga, H., Ogawa, T., Kai, K., Suzuki, H., Ogata, Y., Sakurai, N., Shibata, D., Ohta, D. (2012). Identification and characterization of ANAC042, a transcription factor family gene involved in the regulation of camalexin biosynthesis in Arabidopsis. *Molecular Plant-Microbe Interactions*, *25*(5): 684-696.

Sakuraba, Y., Jeong, J., Kang, M. Y., Kim, J., Paek, N. C., Choi, G. (2014). Phytochrome-interacting transcription factors PIF4 and PIF5 induce leaf senescence in Arabidopsis. *Nature Communications*, *5*(4636): 1-13.

Schmid, N. B., Giehl, R. F. H., Döll, S., Mock, H. P., Strehmel, N., Scheel, D., Kong, X., Hider, R. C., Von Wirén, N. (2014). Feruloyl-CoA 6′-Hydroxylase1-dependent coumarins mediate iron acquisition from alkaline substrates in Arabidopsis. *Plant Physiology*, *164*(1): 160-172.

Schramm, F., Larkindale, J., Kiehlmann, E., Ganguli, A., Englich, G., Vierling, E., Von Koskull-Döring, P. (2008). A cascade of transcription factor DREB2A and heat stress transcription factor HsfA3 regulates the heat stress response of Arabidopsis. *Plant Journal*, *53*(2): 264-274.

Schuhegger, R., Nafisi, M., Mansourova, M., Petersen, B. L., Olsen, C. E., Svatoš, A., Halkier, B. A., Glawischnig, E. (2006). CYP71B15 (PAD3) catalyzes the final step in camalexin biosynthesis. *Plant Physiology*, *141*(4): 1248-1254.

Seo, J. Y., Kim, B. R., Oh, J., Kim, J. S. (2018). Soybean-derived phytoalexins improve cognitive function through activation of Nrf2/HO-1 signaling pathway. *International Journal of Molecular Sciences*, *19*(1): 680-691.

Shahnejat-Bushehri, S., Mueller-Roeber, B., Balazadeh, S. (2012). Arabidopsis NAC transcription factor JUNGBRUNNEN1 affects thermomemoryassociated genes and enhances heat stress tolerance in primed and unprimed conditions. *Plant Signaling and Behavior*, *7*(12): 1518-1521.

Silva, C. S., Nayak, A., Lai, X., Hutin, S., Hugouvieux, V., Jung, J. H., López-Vidriero, I., Franco-Zorrilla, J. M., Panigrahi, K. C. S., Nanao, M. H., Wigge, P. A., Zubieta, C. (2020). Molecular mechanisms of Evening Complex activity in Arabidopsis. *Proceedings of the National Academy of Sciences of the United States of America*, *117*(12): 6901-6909.

Smith, B., Randle, D., Mezencev, R., Thomas, L. S., Hinton, C., Odero-Marah, V. (2014). Camalexin-induced apoptosis in prostate cancer cells involves alterations of expression and activity of lysosomal protease cathepsin d. *Molecules*, *19*(4): 3988-4005.

Solano, R., Stepanova, A., Chao, Q., Ecker, J. R. (1998). Nuclear events in ethylene signaling: A transcriptional cascade mediated by ETHYLENE-INSENSITIVE3 and ETHYLENE-RESPONSE-FACTOR1. *Genes and Development*, *12*(23): 3703–3714.

Song, S., Huang, H., Gao, H., Wang, J., Wu, D., Liu, X., Yang, S., Zhai, Q., Li, C., Qi, T., Xie, D. (2014). Interaction between MYC2 and ETHYLENE INSENSITIVE3 modulates antagonism between jasmonate and ethylene signaling in Arabidopsis. *Plant Cell*, *26*(1): 128903.

Speeckaert, N., Adamou, N. M., Hassane, H. A., Baldacci-Cresp, F., Mol, A., Goeminne, G., Boerjan, W., Duez, P., Hawkins, S., Neutelings, G., Hoffmann, T., Schwab, W., El Jaziri, M., Behr, M., Baucher, M. (2020). Characterization of the udp-glycosyltransferase ugt72 family in poplar and identification of genes involved in the glycosylation of monolignols. *International Journal of Molecular Sciences*, *21*(14): 5018.

Staswick, P. E. (2008). JAZing up jasmonate signaling. *Trends in Plant Science*, *13*(2): 66-71.

Sun, T., Huang, J., Xu, Y., Verma, V., Jing, B., Sun, Y., Ruiz Orduna, A., Tian, H., Huang, X., Xia, S., Schafer, L., Jetter, R., Zhang, Y., Li, X. (2020). Redundant CAMTA Transcription Factors Negatively Regulate the Biosynthesis of Salicylic Acid and N-Hydroxypipecolic Acid by Modulating the Expression of SARD1 and CBP60g. *Molecular Plant*, *13*(1): 144-156.

Sun, Y., Li, L., Macho, A. P., Han, Z., Hu, Z., Zipfel, C., Zhou, J. M., Chai, J. (2013). Structural basis for flg22-induced activation of the Arabidopsis FLS2-BAK1 immune complex. *Science*, *342*(6158): 624-628.

Sung, J., Lee, S., Lee, Y., Ha, S., Song, B., Kim, T., Waters, B. M., Krishnan, H. B. (2015). Metabolomic profiling from leaves and roots of tomato (Solanum lycopersicum L.) plants grown under nitrogen, phosphorus or potassium-deficient condition. *Plant Science*, *10*(1): 1700219.

Suzuki, N., Sejima, H., Tam, R., Schlauch, K., Mittler, R. (2011). Identification of the MBF1 heat-response regulon of Arabidopsis thaliana. *Plant Journal*, *66*(5): 844-851.

Takahashi, F., Yoshida, R., Ichimura, K., Mizoguchi, T., Seo, S., Yonezawa, M., Maruyama, K., Yamaguchi-Shinozaki, K., Shinozakia, K. (2007). The mitogen-activated protein kinase cascade MKK3-MPK6 is an important part of the jasmonate signal transduction pathway in Arabidopsis. *Plant Cell*, *19*(3): 805–818.

Tanaka, Y., Data, E. S., Hirose, S., Taniguchi, T., Uritani, I. (1983). Biochemical changes in secondary metabolites in wounded and deteriorated cassava roots. *Agricultural and Biological Chemistry*, *47*(4): 693-700.

Taylor-Teeples, M., Lin, L., De Lucas, M., Turco, G., Toal, T. W., Gaudinier, A., Young, N. F., Trabucco, G. M., Veling, M. T., Lamothe, R., Handakumbura, P. P., Xiong, G., Wang, C., Corwin, J., Tsoukalas, A., Zhang, L., Ware, D., Pauly, M., Kliebenstein, D. J., Dehesh, K., Tagkopoulos, I., Breton, G., Pruneda-Paz, J. L., Ahnert, S. E., Kay, S. A., Hazen, S. P., Brady, S. M. (2015). An Arabidopsis gene regulatory network for secondary cell wall synthesis. *Nature*, *517*(7536): 571–575.

Thines, B., Katsir, L., Melotto, M., Niu, Y., Mandaokar, A., Liu, G., Nomura, K., He, S. Y., Howe, G. A., Browse, J. (2007). JAZ repressor proteins are targets of the SCFCOI1 complex during jasmonate signalling. *Nature*, *448*(7154): 661-665.

Tobimatsu, Y., Schuetz, M. (2019). Lignin polymerization: how do plants manage the chemistry so well? *Current Opinion in Biotechnology*, *56*: 75-81.

Ton, J., Van Pelt, J. A., Van Loon, L. C., Pieterse, C. M. J. (2002). Differential effectiveness of salicylate-dependent and jasmonate/ethylene-dependent induced resistance in Arabidopsis. *Molecular Plant-Microbe Interactions*, *15*(1): 27-34.

Torres, M. A., Dangl, J. L., Jones, J. D. G. (2002). Arabidopsis gp91phox homologues Atrbohd and Atrbohf are required for accumulation of reactive oxygen intermediates in the plant defense response. *Proceedings of the National Academy of Sciences of the United States of America*, *99*(1): 517-522.

Turner, J. G., Ellis, C., Devoto, A. (2002). The jasmonate signal pathway. *Plant Cell*, *14*: 153-164.

Vanholme, R., Demedts, B., Morreel, K., Ralph, J., Boerjan, W. (2010). Lignin biosynthesis and structure. *Plant Physiology*, *153*(3): 895-905.

Wang, D., Amornsiripanitch, N., Dong, X. (2006). A genomic approach to identify regulatory nodes in the transcriptional network of systemic acquired resistance in plants. *PLoS Pathogens*, *2*(11): 123.

Wang, H. Z., Dixon, R. A. (2012). On-off switches for secondary cell wall biosynthesis. *Molecular Plant*, *5*(2): 297-303.

Wang, P., Zhao, Y., Li, Z., Hsu, C. C., Liu, X., Fu, L., Hou, Y. J., Du, Y., Xie, S., Zhang, C., Gao, J., Cao, M., Huang, X., Zhu, Y., Tang, K., Wang, X., Tao, W. A., Xiong, Y., Zhu, J. K. (2018). Reciprocal Regulation of the TOR Kinase and ABA Receptor Balances Plant Growth and Stress Response. *Molecular Cell*, *69*(1): 100-112.

Wang, W., Feng, B., Zhou, J. M., Tang, D. (2020). Plant immune signaling: Advancing on two frontiers. *Journal of Integrative Plant Biology*, *62*(1): 2-24.

Wang, Y., Chantreau, M., Sibout, R., Hawkins, S. (2013). Plant cell wall lignification and monolignol metabolism. *Frontiers in Plant Science*, *4*: 220.

Widemann, E., Miesch, L., Lugan, R., Holder, E., Heinrich, C., Aubert, Y., Miesch, M., Pinot, F., Heitz, T. (2013). The amidohydrolases IAR3 and ILL6 contribute to jasmonoyl-isoleucine hormone turnover and generate 12-hydroxyjasmonic acid upon wounding in arabidopsis leaves. *Journal of Biological Chemistry*, *288*(44): 6296-6306.

Wu, A., Allu, A. D., Garapati, P., Siddiqui, H., Dortay, H., Zanor, M. I., Asensi-Fabado, M. A., Munná-Bosch, S., Antonio, C., Tohge, T., Fernie, A. R., Kaufmann, K., Xue, G. P., Mueller-

Roeber, B., Balazadeh, S. (2012). JUNGBRUNNEN1, a reactive oxygen species-responsive NAC transcription factor, regulates longevity in Arabidopsis. *Plant Cell*, *24*(2): 482-506.

Xu, G., Yuan, M., Ai, C., Liu, L., Zhuang, E., Karapetyan, S., Wang, S., Dong, X. (2017). UORF-mediated translation allows engineered plant disease resistance without fitness costs. *Nature*, *545*(7655): 491-494.

Yang, Y., Wang, G., Wu, W., Yao, S., Han, X., He, D., He, J., Zheng, G., Zhao, Y., Cai, Z., Yu, R. (2018). Camalexin induces apoptosis via the ROS-ER stress-mitochondrial apoptosis pathway in AML cells. *Oxidative Medicine and Cellular Longevity*, *2018*: 7426950.

Yi, G. E., Robin, A. H. K., Yang, K., Park, J. I., Hwang, B. H., Nou, I. S. (2016). Exogenous methyl jasmonate and salicylic acid induce subspecies-specific patterns of glucosinolate accumulation and gene expression in Brassica oleracea L. *Molecules*, *21*(10): 1417.

Yoshida, T., Sakuma, Y., Todaka, D., Maruyama, K., Qin, F., Mizoi, J., Kidokoro, S., Fujita, Y., Shinozaki, K., Yamaguchi-Shinozaki, K. (2008). Functional analysis of an Arabidopsis heat-shock transcription factor HsfA3 in the transcriptional cascade downstream of the DREB2A stress-regulatory system. *Biochemical and Biophysical Research Communications*, *368*(3): 515-521.

Yoshikawa, M. (1978). Diverse modes of action of biotic and abiotic phytoalexin elicitors [19]. *Nature*, *275*(5680): 546–547.

Yoshioka, H., Hino, Y., Iwata, K., Ogawa, T., Yoshioka, M., Ishihama, N., Adachi, H. (2023). Dynamics of plant immune MAPK activity and ROS signaling in response to invaders. *Physiological and Molecular Plant Pathology*, *125*: 102000.

Zhai, Q., Zhang, X., Wu, F., Feng, H., Deng, L., Xu, L., Zhang, M., Wang, Q., Li, C. (2015). Transcriptional mechanism of jasmonate receptor COI1-mediated delay of flowering time in arabidopsis. *Plant Cell*, *27*(10): 2814-2828.

Zheng, Z., Qamar, S. A., Chen, Z., Mengiste, T. (2006). Arabidopsis WRKY33 transcription factor is required for resistance to necrotrophic fungal pathogens. *Plant Journal*, *48*(4): 592-605.

Zhou, J., Mu, Q., Wang, X., Zhang, J., Yu, H., Huang, T., He, Y., Dai, S., Meng, X. (2022). Multilayered synergistic regulation of phytoalexin biosynthesis by ethylene, jasmonate, and MAPK signaling pathways in Arabidopsis. *Plant Cell*, *34*(8): 3066–3087.

Zhou, J., Wang, X., He, Y., Sang, T., Wang, P., Dai, S., Zhang, S., Meng, X. (2020). Differential phosphorylation of the transcription factor WRKY33 by the protein kinases CPK5/CPK6 and MPK3/MPK6 cooperatively regulates camalexin biosynthesis in arabidopsis. *Plant Cell*, *32*(8): 2621-2638.

Zhu, Z., An, F., Feng, Y., Li, P., Xue, L., A, M., Jiang, Z., Kim, J. M., To, T. K., Li, W., Zhang, X., Yu, Q., Dong, Z., Chen, W. Q., Seki, M., Zhou, J. M., Guo, H. (2011). Derepression of ethylene-

stabilized transcription factors (EIN3/EIL1) mediates jasmonate and ethylene signaling synergy in Arabidopsis. *Proceedings of the National Academy of Sciences of the United States of America*, *108*(30): 12539-12544.

APPENDIX A: SUPPLEMENTAL TABLES (PRIMERS AND COMPOUND IONIZATION)

Table S1. List of primer names, nucleotide sequences (5' to 3'), and their intended experimental applications used in this study.

Oligo Name	Sequence (5' to 3')	Purpose
cANACf	CTTCCTGGGTTCAGGTTTCA	Cloning
cANACr	ACCAAGCAGCTTAGATTCCG	Cloning
HSF6-1f	AAAAAGCAGGCTTAACAATGGAAGGAACAAGTGAAAAGG	Cloning
HSF6-1r	TTGTCTCAGTCATGCAAATAGCTCACCCAGCTTTCT	Cloning
Att_HSF6f	GGGGACAAGTTTGTACAAAAAAGCAGGCTAACCATGGAAGGAACAAGTGAAAAGG	Cloning
P2A_HSF6r	ATGTTGTCTCAGTCATGCAAAGGATCCGGAGCCACGAACTTCTCTCTGTTAAAGCAAGCAGGAGAC	Cloning
P2A-M29A2f	GCCACGAACTTCTCTCTGTTAAAGCAAGCAGGAGACGTGGAAGAAAACCCCGGTCTTATGGTTAGAGCTCCTTGTTGTGAA	Cloning
Att_M29A2r	ATCGAATTGCCAGAGTTCTGATACCCAGCTTTCT	Cloning
pDESTnF	AGAAAGCTTAAGGCGGGAAACGACAAT	Cloning
pDESTnR	GGAGTCACGTTATGAAGGCCAAGCTTTCT	Cloning
siJAZ1-9f	AAAAAGCAGGCTGCTGCTCAGTTGACGATGTT	Cloning
siJAZ1-9r	CCAAGCACCCTATCAAATAAACACCCAGCTTTCT	Cloning
cAtM15f	TAAACGTGGCAATTTCACCA	PCR
cAtM15r	AACTTTTGGTGCGGATATCG	PCR
c29A2f	CTTGGACCCCAGAGGAAGA	PCR
c29A2r	ATTAAGGTGTGGCAAGAGCTG	PCR
cHSF6-1f	ATGGAAGGAACAAGTGAAAAGG	PCR
cHSF6-1r	GAAGGAGAATGGGGTGTTGA	PCR
P2Aseq3p	TCTGTTAAAGCAAGCAGGAGAC	Sequencing
P2Aseq5p	TCTGTTAAAGCAAGCAGGAGAC	Sequencing

FMVseq5p	TTCGGTGGATGTCTTTTTCTG	Sequencing
pFMVseq3p	AGCACATGCATCATGGTCAG	Sequencing
p35Sseq3p	CAACCACGTCTTCAAAGCAA	Sequencing
qatjaz1-1f	GCCTGTCTAAATCCCCTTGC	qRT-PCR
qatjaz1-1r	TTTTGTTGACGAACCATACTATCAA	qRT-PCR
qANAC042f	TCTTGGTTCAGCCGGTAAAG	qRT-PCR
qANAC042r	AAAACCGACTCTCCAGCTCA	qRT-PCR
qMYB15f	CTTGGCAATAGATGGTCAGC	qRT-PCR
qMYB15r	GACTCGAAGATTATCAACCA	qRT-PCR
qWRKY33f	TGGAGAGAGCATCACACGAC	qRT-PCR
qWRKY33r	TTACGCCACAAACAGAGCAC	qRT-PCR
qEMB1144f	CGTACCCAAACCAGGAAGAA	qRT-PCR
qEMB1144r	CACATGGAGGAGGAGTTGGT	qRT-PCR
qFOX1f	AGCTGGCTTAACACGACGTT	qRT-PCR
qFOX1r	TACGTCAAAAAGCCAATCCC	qRT-PCR
qCYP71A12f	GAGGCTTCCGTTGATTGGTA	qRT-PCR
qCYP71A12r	CTTCGGTACGGACCACTCAT	qRT-PCR
qCYP79B2f	CAACCGAAACATCGTCCTTT	qRT-PCR
qCYP79B2r	AAATTGATGACGGATCCCAA	qRT-PCR
qCYP82C2f	CCATCGAGAGGCGATAGAAG	qRT-PCR
qCYP82C2r	ATCCAAAGAGATCCGAGGGT	qRT-PCR
qPAL1f	GGAATATTCGGAAGCACGAA	qRT-PCR
qPAL1r	TTTCCGGTATCCGATTTGAG	qRT-PCR
qCYP71B15f	CGGAAGAATCGGTAGGTTCA	qRT-PCR
qCYP71B15r	ACGAGCATCTTAAGCCTGGA	qRT-PCR
qCYP71A13f	TAGATGGGATCCGTGGTTTC	qRT-PCR
qCYP71A13r	GATAAAGCGGATTTCGTGGA	qRT-PCR
qMYB15f	CTTGGCAATAGATGGTCAGC	qRT-PCR
qMYB15r	GACTCGAAGATTATCAACCA	qRT-PCR
qSK1f	ACGACCACTGCTACACGATG	qRT-PCR

qSK1r	CATACACAAACGCAAATGCC	qRT-PCR
qSK2f	ATTATGGCAAGATCGTTGG	qRT-PCR
qSK2r	TGAGCATTTCGGTGAGAGTG	qRT-PCR
qCYP79B3f	CGTGGCACTCTCTGATACGA	qRT-PCR
qCYP79B3r	TAACCCCAAGGTTTGGTCTG	qRT-PCR
qUBQ10f	GTTGGAGGATGGCAGAACTC	qRT-PCR
qUBQ10r	CGTTAAGACGTTGACTGGGA	qRT-PCR

Table S2. Compounds detected in negative ionization mode by MALDI-HRMS, including their deprotonated molecular formulas, and deprotonated mass-to-charge ratios (*m/z*) with charge state. Metabolites were identified based on a 5 parts per million (ppm) mass error.

Compound Name	**Deprotonated Molecular Formula**	**[M-H] (*m/z*)**	**Charge State**
Monolignol H	C_9H_8O	[149.0614]	(-)
Phenylalanine	$C_9H_{10}NO_2$	[164.0712]	(-)
Monolignol C	$C_{10}H_{11}O_3$	[165.056]	(-)
Caffeic Acid	$C_9H_8O_4$	[179.0344]	(-)
Monolignol G	$C_{10}H_{10}O_2$	[179.0717]	(-)
4OH-ICN	$C_{10}H_5N_2O_2$	[185.0361]	(-)
IAOx	$C_{10}H_9N_2O_2$	[189.0664]	(-)
Scopoletin	$C_{10}H_7O_4$	[191.035]	(-)
Monolignol 5H	$C_{10}H_{11}O_4$	[195.0669]	(-)
Camalexin	$C_{11}H_7N_2S$	[199.0333]	(-)
Tryptophan	$C_{11}H_{11}N_2O_2$	[203.082]	(-)
Monolignol S	$C_{11}H_{13}O_4$	[209.082]	(-)
Chorismate	$C_{10}H_9O_6$	[225.0399]	(-)
Daidzein (Internal Standard)	$C_{15}H_9O_4$	[253.0501]	(-)

Table S3. The soybean transcription factors with their corresponding accession numbers.

TF Name	Accession Number
GmMYB29A2	Glyma.02G005600
GmHSF6-1	Glyma.03G135800
GmJAZ1-9	Glyma.13G112000

APPENDIX B: SUPPLEMENTAL FIGURE

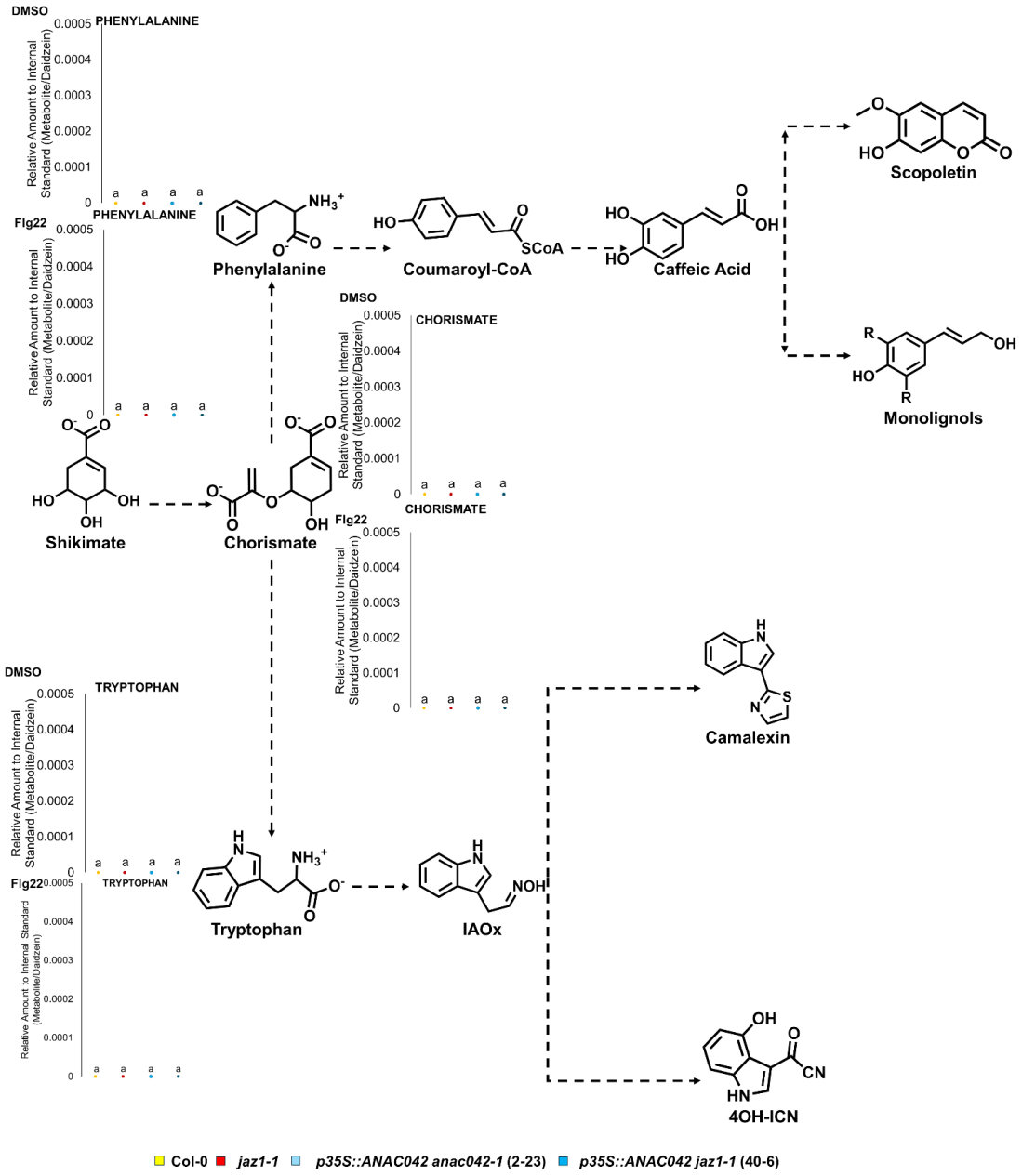

Figure S1. *ANAC042* overexpression in *jaz1-1* influences phytoalexin biosynthesis precursors. Metabolite precursors from primary metabolism and precursors that lead to Trp- and Phe-derived metabolites in Arabidopsis seedling extracts treated for 10 days with DMSO and Flg22. These were quantified by MALDI-HRMS and the different letters show significant differences by single factor ANOVA, Tukey post-hoc test, $p < 0.01$, $\alpha = 0.05$. Error bars represent standard error (SE), $n = 3$ per treatment.

APPENDIX C: Soybean Constructs

Construction of pGEMINI-B

To construct *pGEMINI-B*, the full-length attB1/attB2 Gateway cassette, including the *figwort mosaic virus* (*FMV*) promoter from the *pGEMINI* vector, was amplified by PCR using pDESTnF/R primers (Table S1). The resulting amplicon contains not only contains the attB1/attB2 Gateway cassette, but possess HindIII restriction sites at both terminal ends of the fragment. This fragment was digested overnight using HindIII (New England Biolabs, MA, USA), alongside with *pGWB602* to linearize the plasmid at 37°C. The linearized *pGWB602* plasmid was dephosphorylated with Antarctic phosphatase (New England Biolabs, MA, USA) at 37°C for one hour. The Gateway cassette was then ligated into *pGWB602* to form *pGEMINI-B*. This new plasmid contains the *aadA* and *bar* genes for resistance to spectinomycin in bacteria and phosphinothricin in plants, respectively. To verify the insertion of the Gateway cassette, an overnight digestion using HindIII was performed and visualized on a 1% agarose gel. Colonies that exhibited two bands, one in the 2000 bp range, were sent for sequencing (The Centre for Applied Genomics, ON, Canada) to ensure fidelity and orientation.

Cloning Soybean TFs

For the soybean constructs, the CDS of *GmMYB29A2* and *GmHSF6-1* were PCR amplified from complementary DNA of hairy roots of *Glycine max* L. merr Williams 82 (W82) (USDA-GRIN Soybean Germplasm Collection, MD, USA). Prior to collection, hairy roots were treated with WGE for 24 hours as described by (Jahan et al., 2020; Lin et al., 2023). The resulting PCR amplicons were cloned into the Gateway entry vector, *pDONR221* (Invitrogen, ON, Canada) using BP Clonase enzyme mix. Amplification of *GmHSF6-1* and *GmMYB29A2* CDSs was carried out using 2X Phusion High-Fidelity Master Mix (ThermoFisher Scientific, MA, USA) following the methods of (Hilgarth and Lanigan, 2020), with primer pairs Att_HSF6f/P2A_HSF6r and P2A-M29A2f/Att_M29A2r, respectively. This procedure generated two fragments. The first fragment contained the Att site, the CDS of *GmHSF6-1*, and the 3' portion of the *P2A* peptide sequence, while the second contained the 5' segments of the *P2A* peptide sequence, the *GmMYB29A2* CDS, and the terminal Att site. These two fragments were fused together through overlap extension PCR to create an in frame *GmHSF6-1-P2A-GmMYB29A2* construct. The full-length fusion was then amplified by PCR using primers

Att_HSF6f/Att_M29A2r. For RNAi of *GmJAZ1* genes, a hairpin was synthesized containing 302 nucleotides of the 5'-CDS of *GmJAZ1-9* arranged inverted orientations flanking the pANDA linker (Miki and Shimamoto, 2004). The resultant *GmHSF6-1-P2A-GmMYB29A2* fusion was recombined into *pGEMINI-B* along with the RNAi-*GmJAZ1-9* hairpin using LR clonase (Invitrogen, ON, Canada). Clones were screened for the presence of *GmHSF6-1-P2A-GmMYB29A2* and the *RNAi-GmJAZ1-9* hairpin by PCR using their respective primers, cHSFf/r, siJAZ1-9f/r, and MYB29A2f/r. The fidelity of these inserts was later confirmed by Sanger sequencing.

Engineering a dual-gene plasmid for combinatorial regulation of glyceollin biosynthesis

The discovery that *ANAC042* overexpression coupled with *JAZ1* knockout unlocks the production of some phytoalexins in Arabidopsis raises important questions about the potential conservation of this regulatory mechanism. To explore further, we designed a single DNA construct to simultaneously co-express positive regulators and silence *JAZ1* genes in soybean. Specifically, a construct to co-overexpress *GmHSF6-1* and *GmMYB29A2* while silencing *GmJAZ1* genes for glyceollin production in soybean. We selected *GmHSF6-1* and *GmMYB29A2* because yeast-one hybrid data from our lab showed that they collectively interact with most glyceollin biosynthetic gene promoters (unpublished data). To enable the simultaneous expression and silencing of multiple genes, I constructed a Gateway-compatible dual-gene expression vector named *pGEMINI-B.* It features two Gateway cassettes arranged in opposite orientations driven by *35S* and *FMV* promoters, respectively (Figure 7A). Using overlap PCR, I fused *GmHSF6-1* and *GmMYB29A2* coding sequences with a P2A self-cleaving peptide, to make a single translational reading frame, and cloned the fusion into the *FMV* site of *pGEMINI-B*. An inverted repeat of 302 bp of *GmJAZ1-9* was synthesized flanking the pANDA linker to make an RNAi silencing cassette, which was recombined into the *35S* site (Miki and Shimamoto, 2004; Figure 7B and 7C). The P2A self-cleaving peptide enables co-translation of *GmHSF6-1* and *GmMYB29A2*, while the pANDA-linker encodes an intron that enhances the processing of RNAi hairpins into small interfering (si)RNA. In future studies, glyceollin accumulation in hairy roots transformed with this multigene construct will be compared to those expressing the individual component genes (Figure 7C). As in Arabidopsis, this system will determine whether combined overexpression and *JAZ1* depletion will increase phytoalexin production.

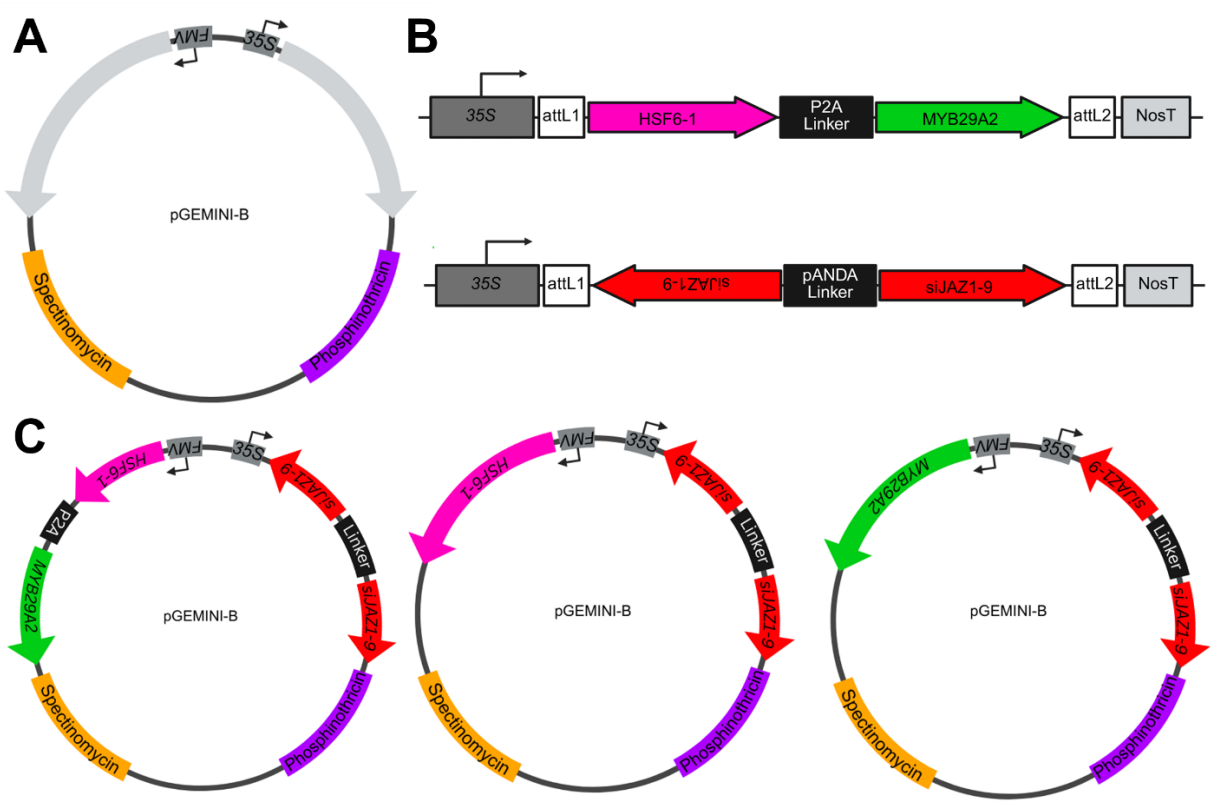

Figure S2. (A) Schematic representation of plasmid, *pGEMINI-B* with two opposing orientation cloning cassette. **(B)** Top shows a P2A self-cleaving peptide situated in between the *GmHSF6-1* and *GmMYB29A2* genes and bottom demonstrates the inverted repeats of silencing *GmJAZ1-9* with a pANDA linker. **(C)** A schematic that shows the final plasmid products with *GmHSF6-1-P2A-GmMYB29A2* driven by *FMV* promoter and RNAi *GmJAZ1-9* under *35S* promoter. These will be tested alongside *GmHSF6-1*/*GmMYB29A2* on one promoter while RNAi *GmJAZ1-9* located in the other.